Understanding the fate of stars:
imaging the surface of red giants and red supergiants*

Heidelberg Joint Astronomy Colloquium

Heidelberg
May 18, 2010

Guy Perrin

l'Observatoire de Paris — LESIA
Laboratoire d'Études Spatiales et d'Instrumentation en Astrophysique

*Special thanks to Steve Ridgway, Xavier Haubois, Pierre Kervella and Sylvestre Lacour

Introduction

The fate of stars

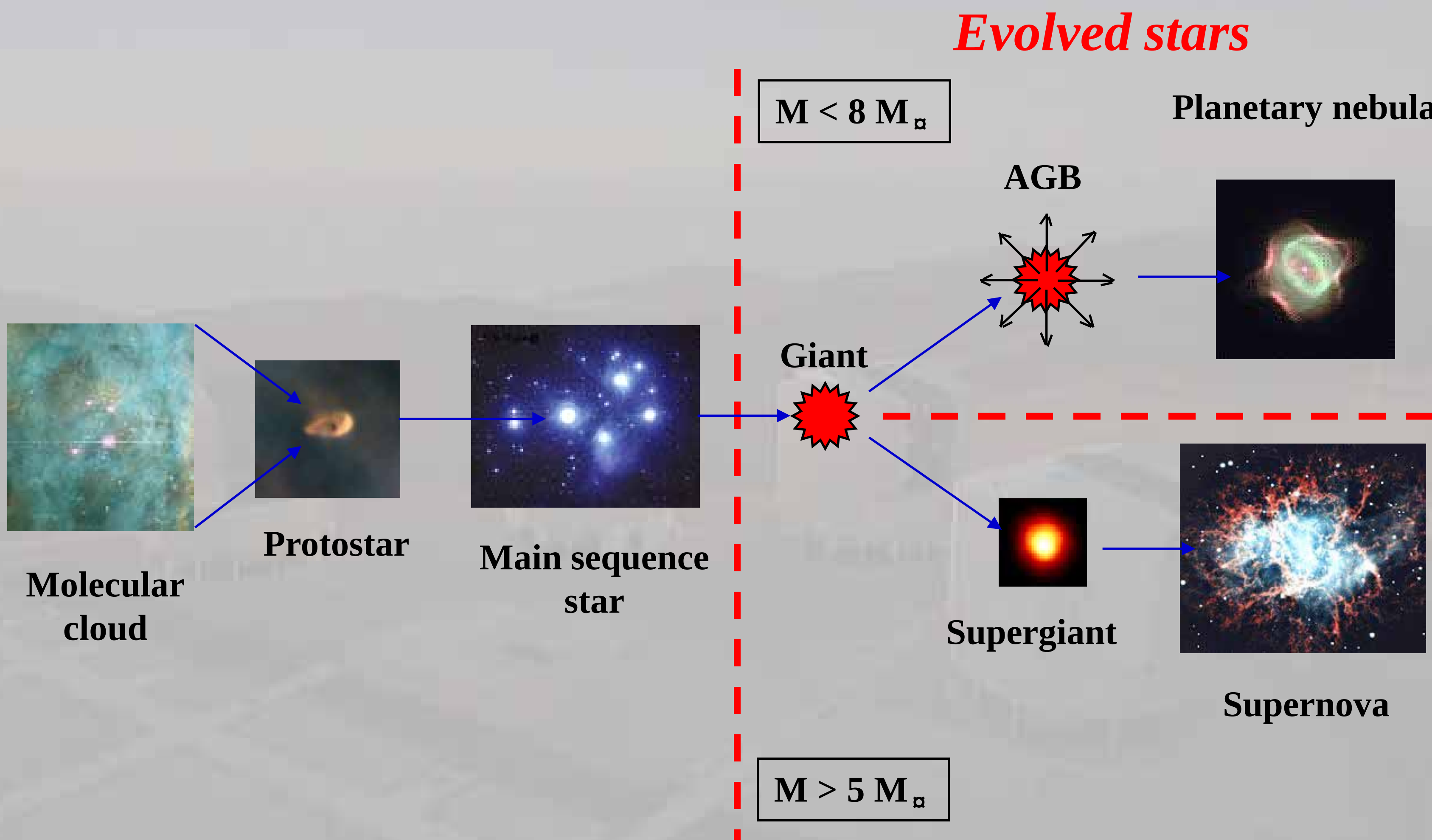

The dust factory

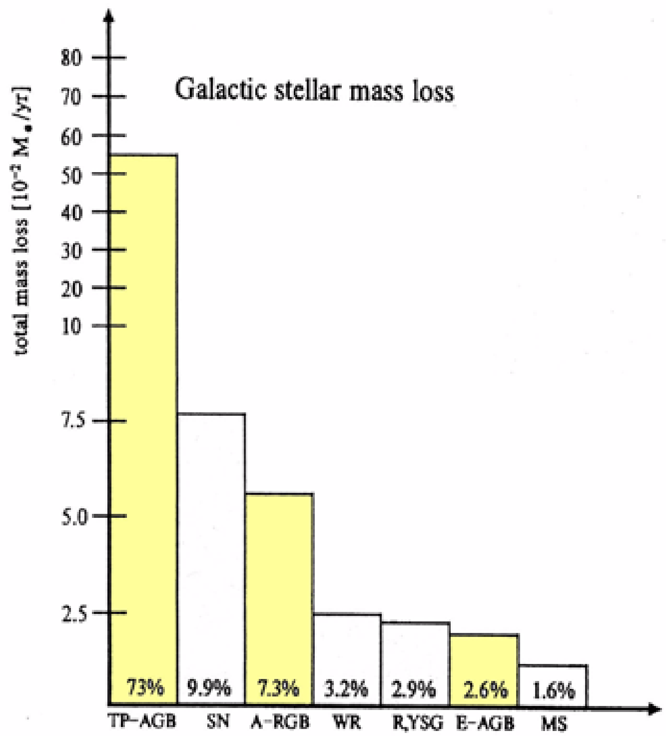

Fig. 1. Total galactic mass loss (solar masses per year) of various classes of stellar objects: TP-AGB: tip-AGB objects, SN: supernovae, A-RGB: asymptotic red giant branch, WR-stars, R, YSG: red and yellow supergiants, E-AGB: early AGB objects, MS: main sequence stars. The indicated numbers are collected from the literature and are inferred from a rather inhomogeneous material (Weinzierl 1991). Despite these inherent uncertainties, they provide a confidential order of magnitude and a clear trend which is expressed at the percentage of their relative contribution to the total mass loss.

Seldmayer (1994)

Two classes of mechanisms for mass loss in evolved stars

- **Low to intermediate mass stars, current paradigm:**
  - pulsations levitate material high enough in the atmosphere to form dust (temperature ~ 1000 K).
  - radiative pressure on grains set them in motion and grains drag the gas away from the star.

- **Higher mass stars (supergiants):**
  - Very high luminosity and low surface gravity: outflow.
  - Other explanation ?

Questions raised by the scenario

- **Stellar surfaces**
  - Smoothness, spots, how many, time and spatial scales, generated by convection?
  - link with mass-loss ?
- **Close stellar environment**
  - Where do the molecules for and where are they?
  - Where and how the does dust form?
- **Pulsation**
  - Is pulsation the only mechanism to invoke?
  - What alternative mechanism for red supergiants?

Questions raised by the scenario

- **Outflows, Post-AGB stars and Planetary Nebulae**
  - Connection with early star history?

Post-AGB

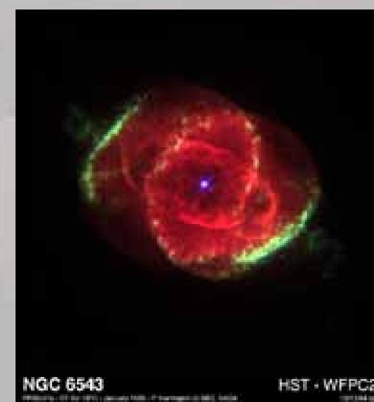

Planetary nebulae

A (*The*) supergiant star: Betelgeuse

QuickTime™ et un
décompresseur TIFF (LZW)
sont requis pour visionner cette image.

Young et al. (2000)

Pupil masking at WHT @ 700nm (continuum)

UV observation with HST

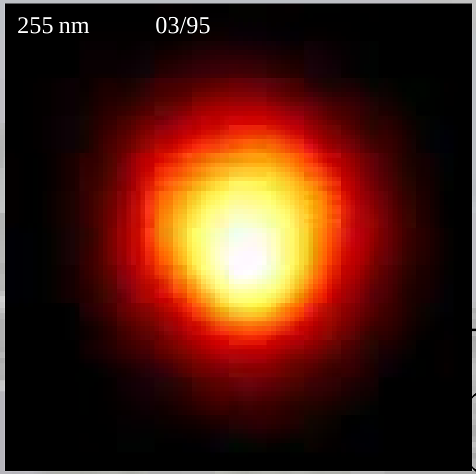

Gilliland & Dupree (1995)

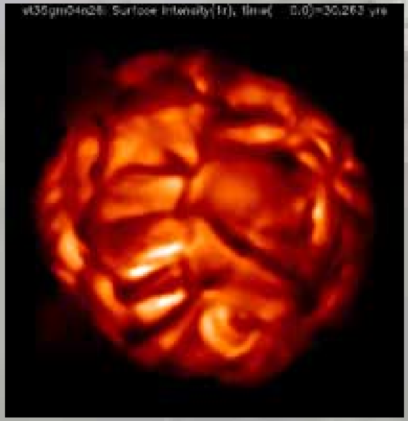

Simulation B. Freytag

Mira stars: R Leo, R Cas & Mira

R Leo

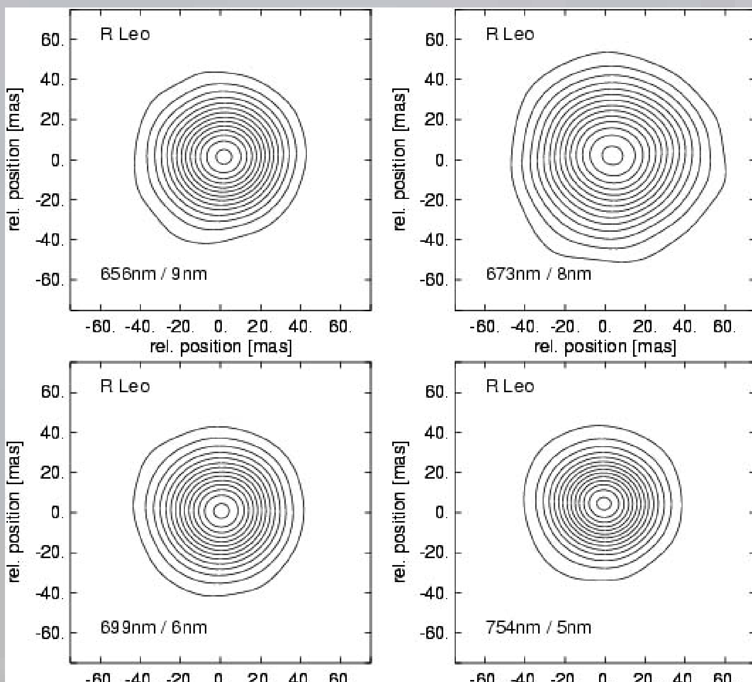

Hofmann et al. (2001, 6m)

R Cas

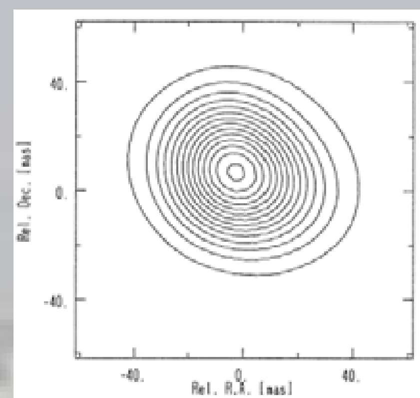

Weigelt et al. (1996, 714 nm, 6m)

Mira
(UV)

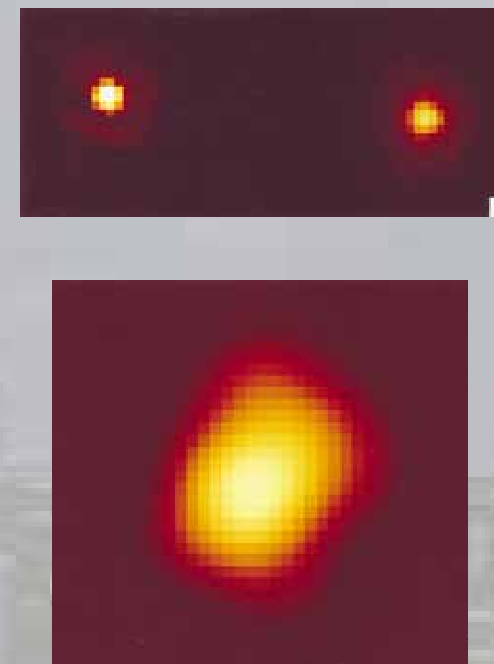

Karovska et al. (1997, HST)

Resolution : 25 mas

Basics of interferometry

Astronomical interferometer

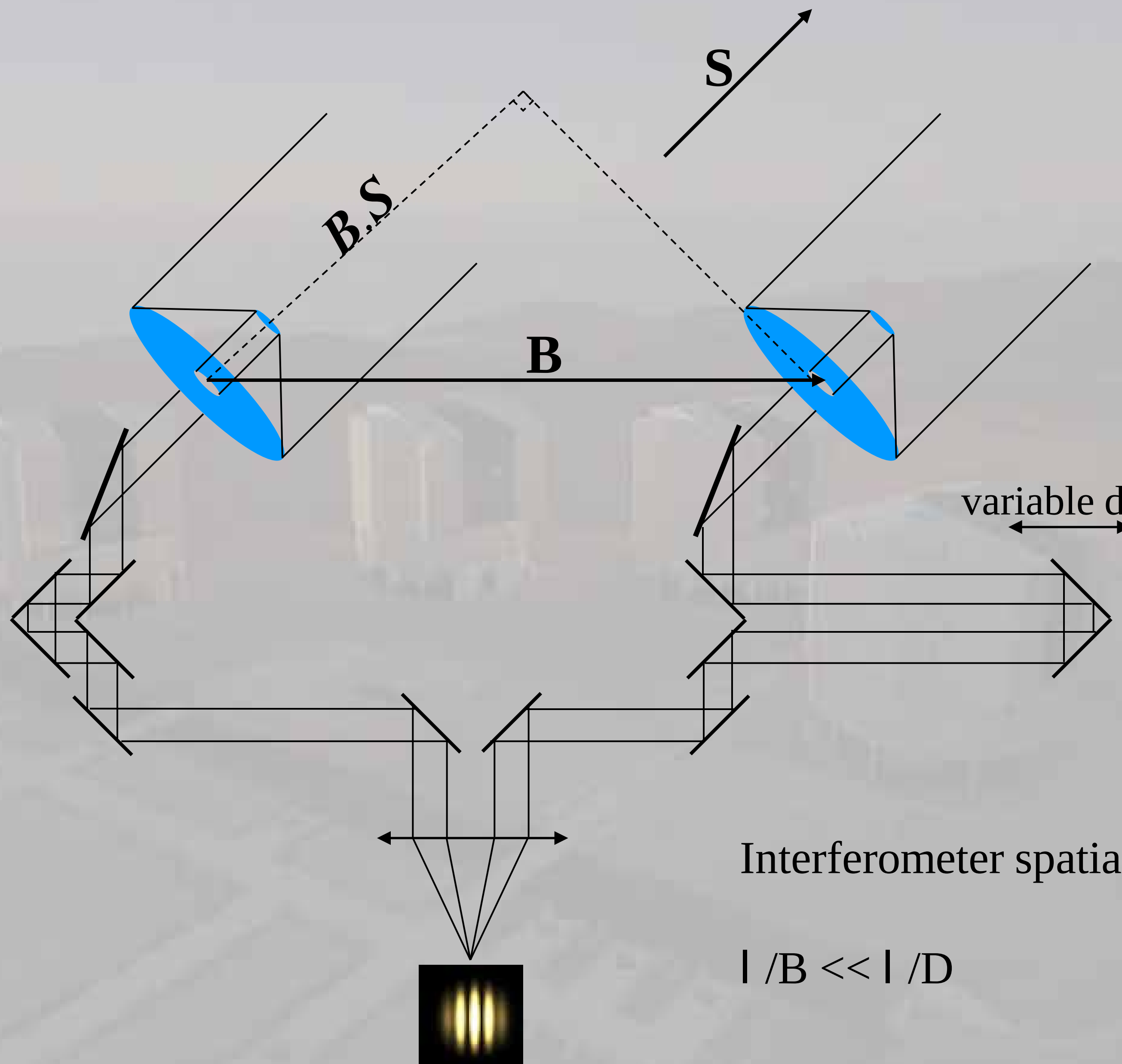

Interferometer spatial resolution:

$\lambda/B \ll \lambda/D$

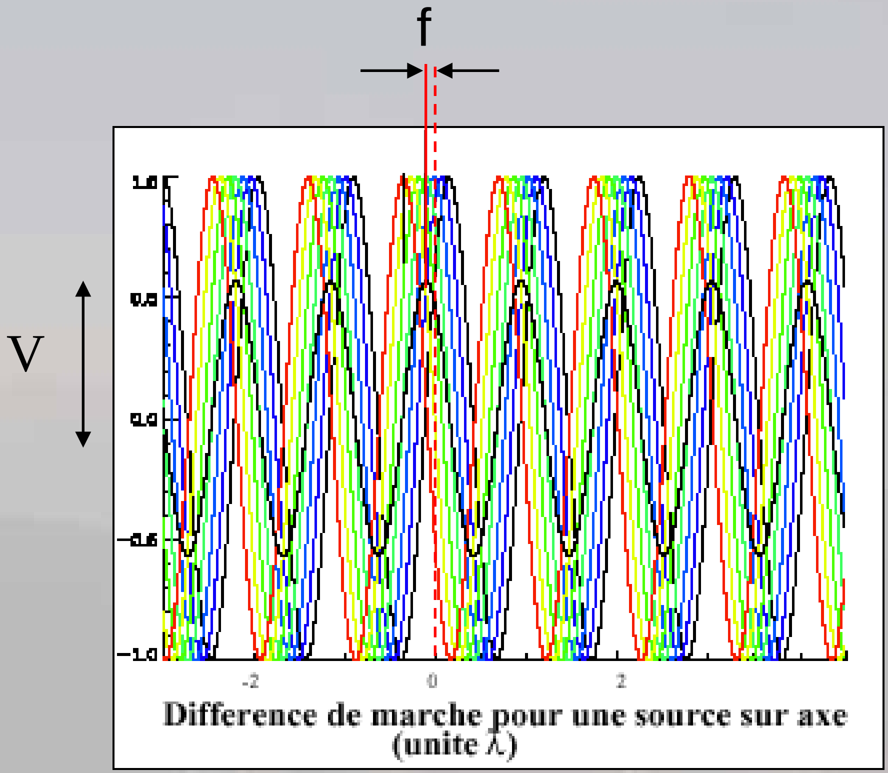

The interferometer measures the ***complex visibility***:

- the modulus is the fringe contrast of the interference pattern

- the phase is derived from the position of the central fringe with respect to the zero optical path difference: $\varphi = \dfrac{2\pi\delta}{\lambda}$

Complex visibility and source spatial brightness distributions are linked by the Zernike - van Cittert theorem:

$$V(B) = \frac{\int_{source} I(S) \exp\left[-2i\pi S.\frac{B}{\lambda}\right] d^2S}{\int_{source} I(S)\, d^2S}$$

Principle of closure phase

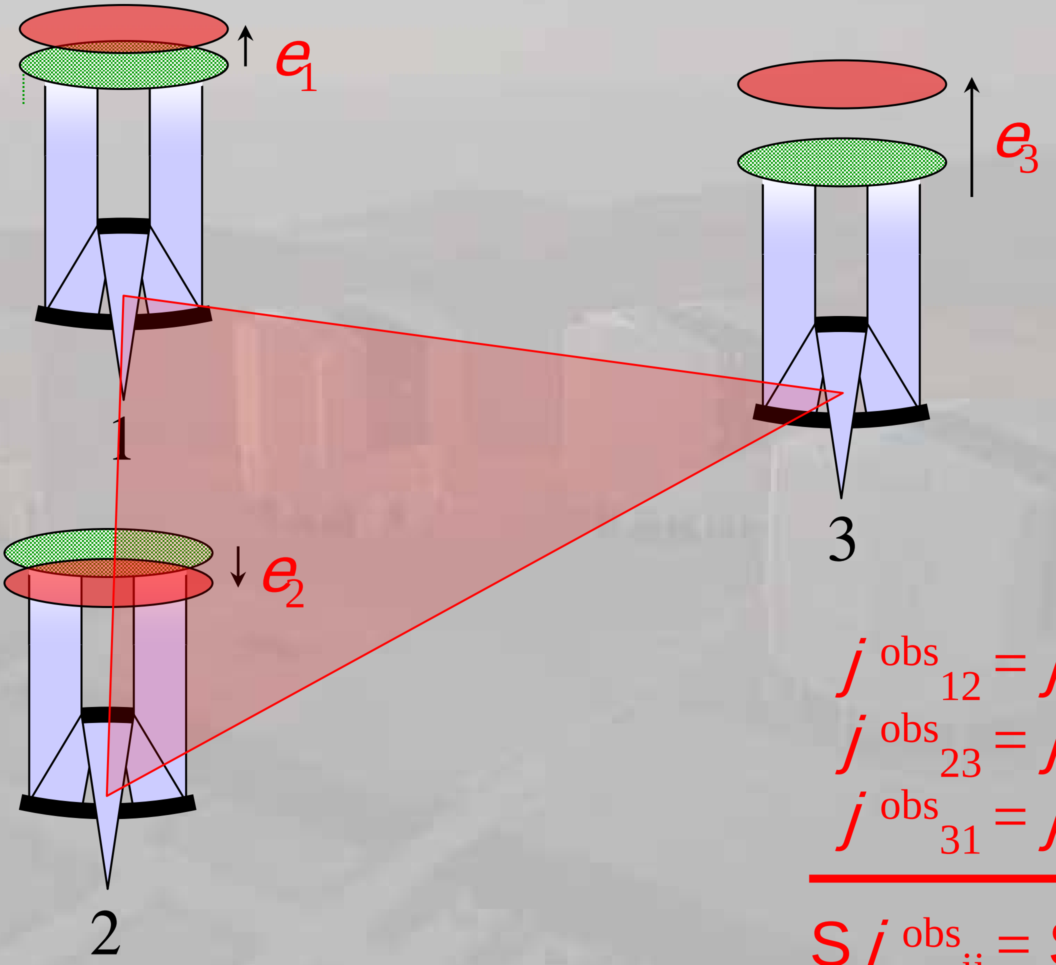

$$\varphi^{\mathrm{obs}}_{12} = \varphi_{12} + \cancel{\varepsilon_1 - \varepsilon_2}$$
$$\varphi^{\mathrm{obs}}_{23} = \varphi_{23} + \cancel{\varepsilon_2 - \varepsilon_3}$$
$$\varphi^{\mathrm{obs}}_{31} = \varphi_{31} + \cancel{\varepsilon_3 - \varepsilon_1}$$

$$\Sigma\,\varphi^{\mathrm{obs}}_{ij} = \Sigma\varphi_{ij}$$

Rules of thumb of interferometry

Fringe contrast (or visibility modulus):
The larger the object, the smaller the visibility (the object gets resolved)

The longer the baseline, the smaller the visibility (resolution = l /B)

Closure phase:
A centro-symmetric object has a 0 (π) closure phase.
Departure from zero is a detection of an asymmetry.

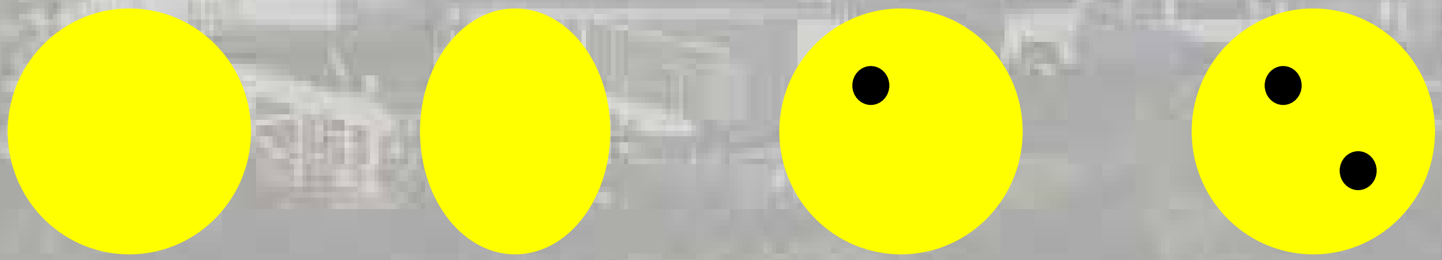

Phase: 0 (π) 0 (π) ≠ 0 (π) 0 (π)

Example: measurement of star diameter with visibilities

Uniform disk: $I(\vec{S}) = \Pi\left(\frac{S}{\theta}\right)$ with θ the disk angular diameter

Visibility function: $V(\vec{B}) = \dfrac{2J_1\left(\frac{\pi\theta B}{\lambda}\right)}{\frac{\pi\theta B}{\lambda}}$

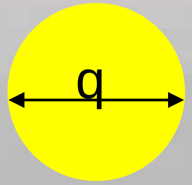

Modulus of the visibility function:

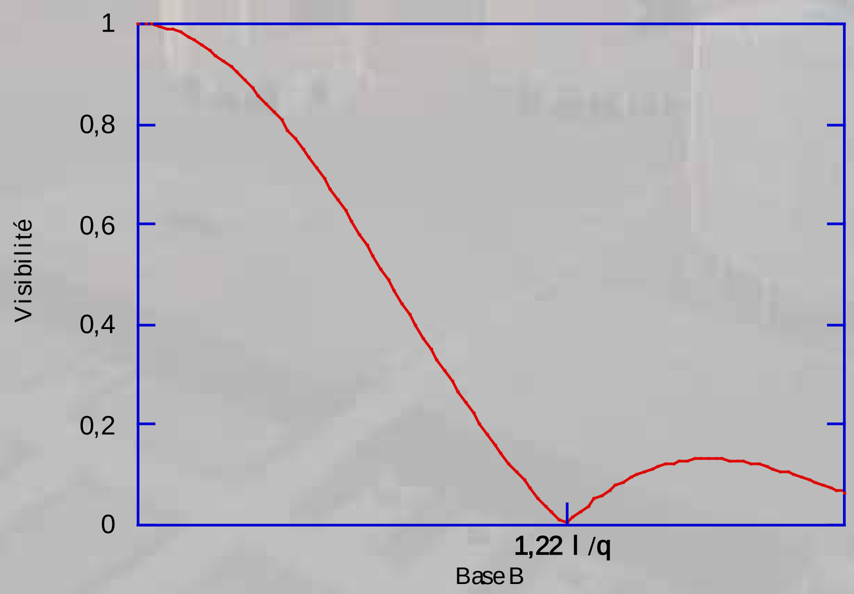

(visibility) Measurements of quiet giant stars

Measurement of limb-darkening

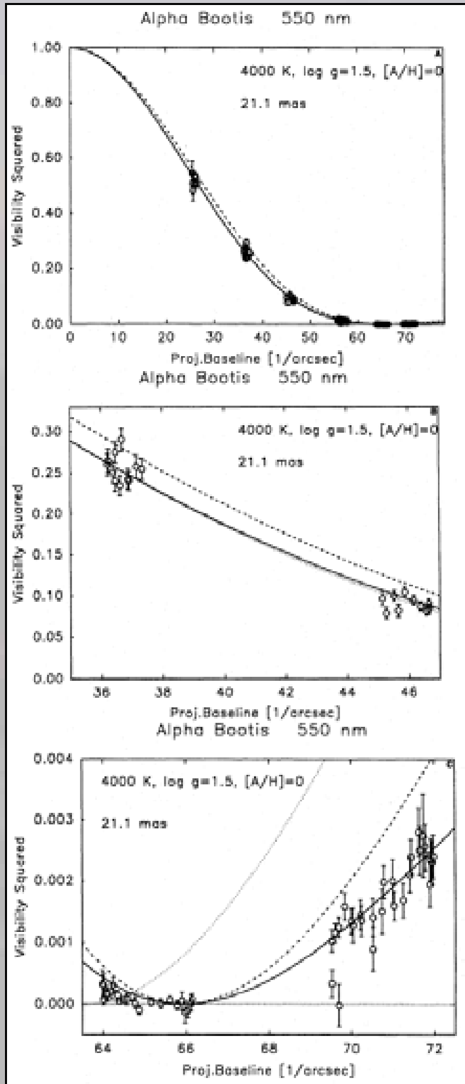

Quirrenbach et al. (1996, Mark III)

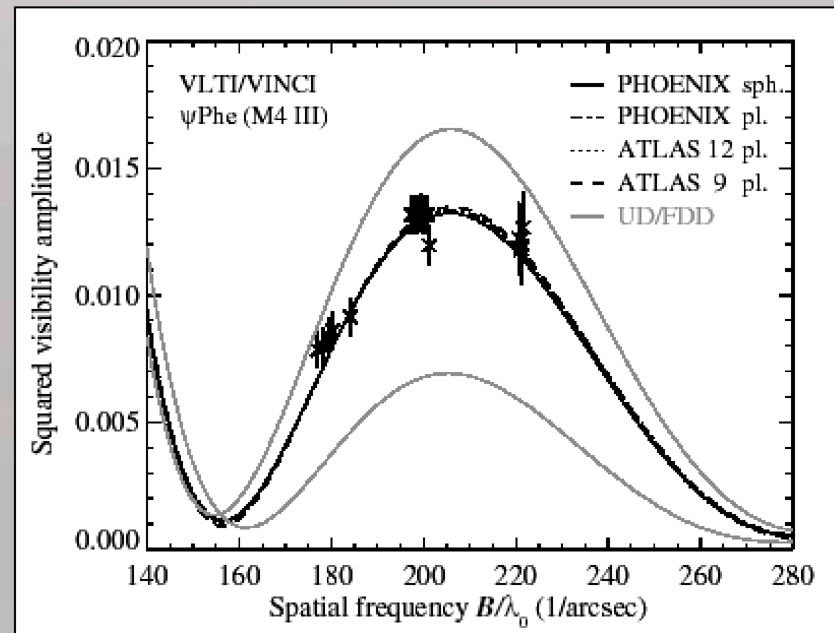

Wittkowski et al. (2004, VINCI)

Limb-darkening measurements provide first order infos on the atmosphere structure and are well explained by atmospheric static models.

The multi-λ study of γ Sge (M0 III)

(Wittkowski et al. 2006)

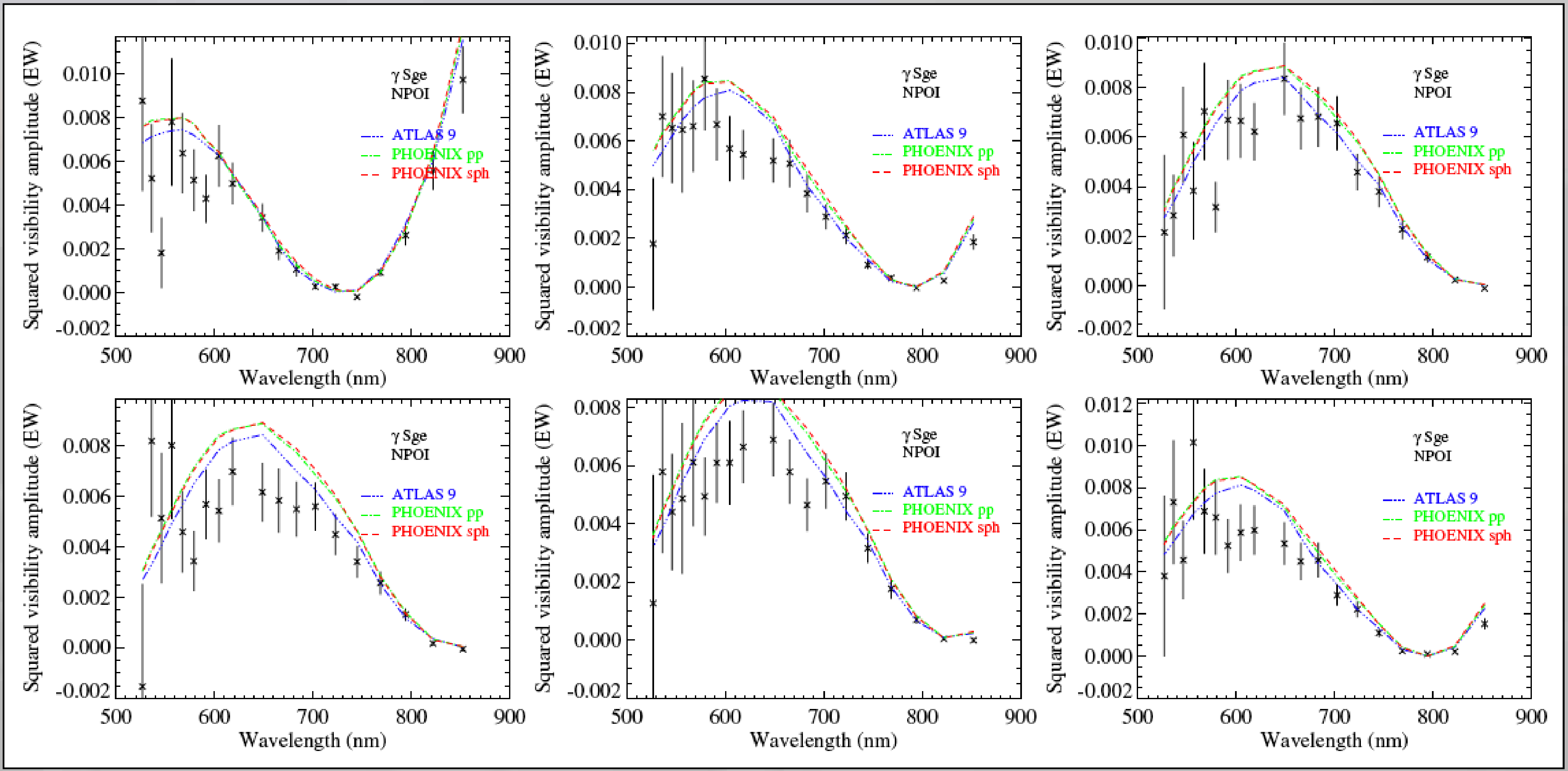

The multi-λ study of γ Sge (M0 III)

(Wittkowski et al. 2006)

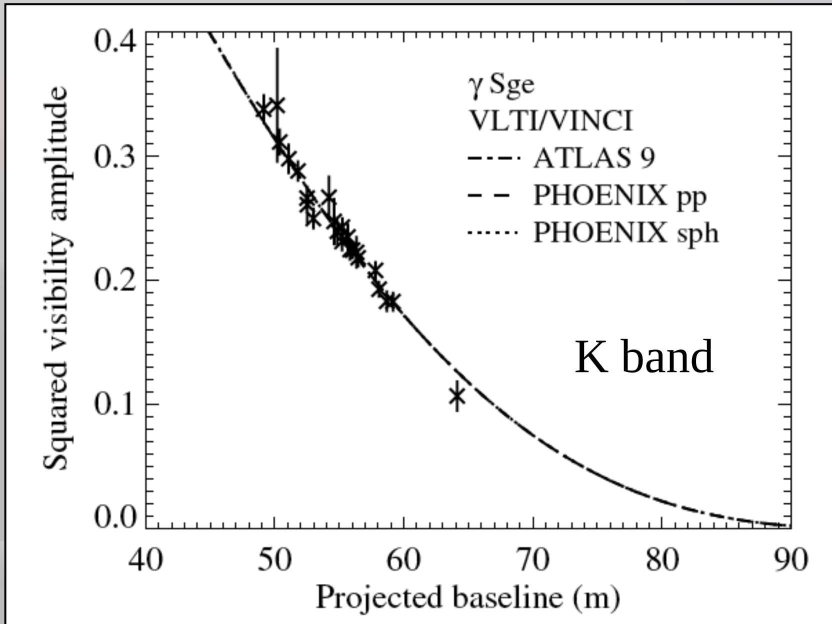

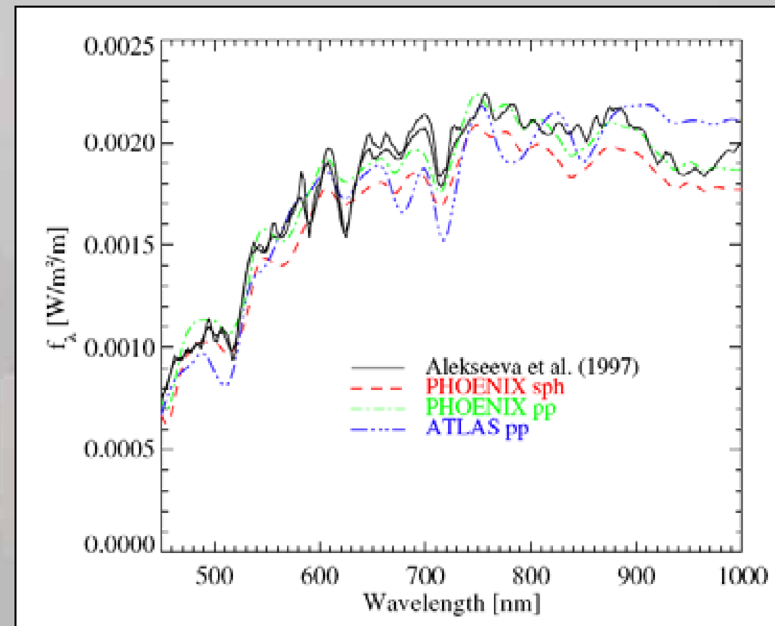

T_{eff}, Mass and log *g* were fixed in the modeling.

The diameter was left as a free parameter.

Global spectrum shape ok but TiO bands remain difficult to model.

Parameter	Value
Rosseland angular diameter	$\Theta_{Ross} = 6.06 \pm 0.02$ mas
Rosseland linear radius	$R_{Ross} = 55 \pm 4\ R_\odot$
Bolometric flux	$f_{bol} = (2.57 \pm 0.13) \times 10^{-9}$ W/m^2
Effective temperature	$T_{eff} = 3805 \pm 55$ K
Luminosity	$\log L/L_\odot = 2.75 \pm 0.08$
Mass	$M = 1.4 \pm 0.4\ M_\odot$
Surface gravity	$\log g = 1.1 \pm 0.2$

Star diameters inside and outside TiO bands

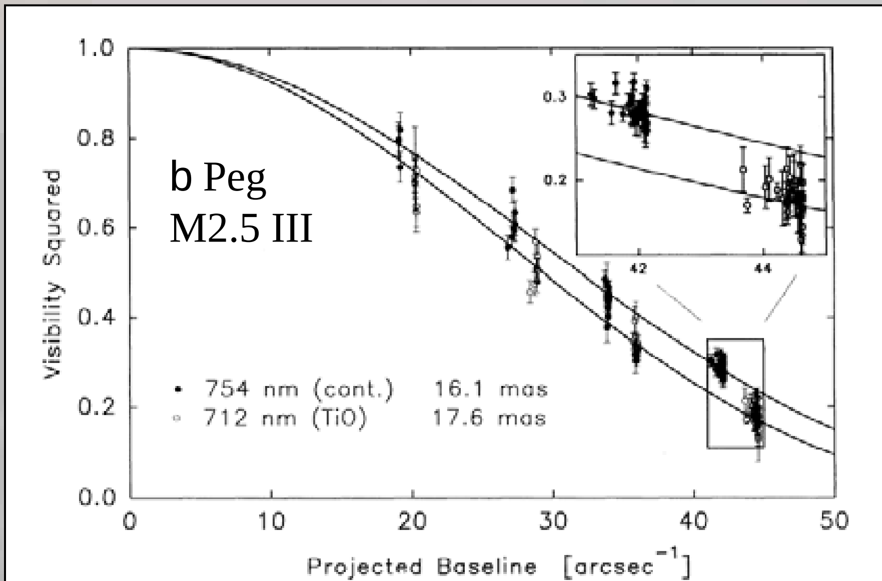

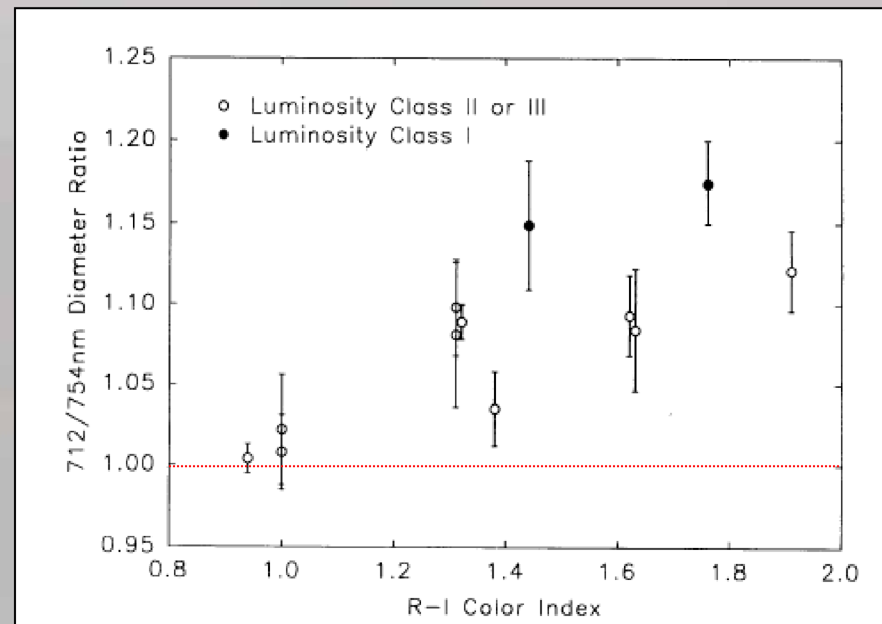

Quirrenbach et al. (1993, Mark III)

The variety of altitudes inside and outside TiO bands is large
Ü the structure of the atmosphere is more complex for later type stars

The MOLsphere of red supergiants*

**MOLsphere* was coined by Tsuji who proposed its existence to explain IR spectra of μ Cep and Betelgeuse.

Molecular layer model: the MOLsphere

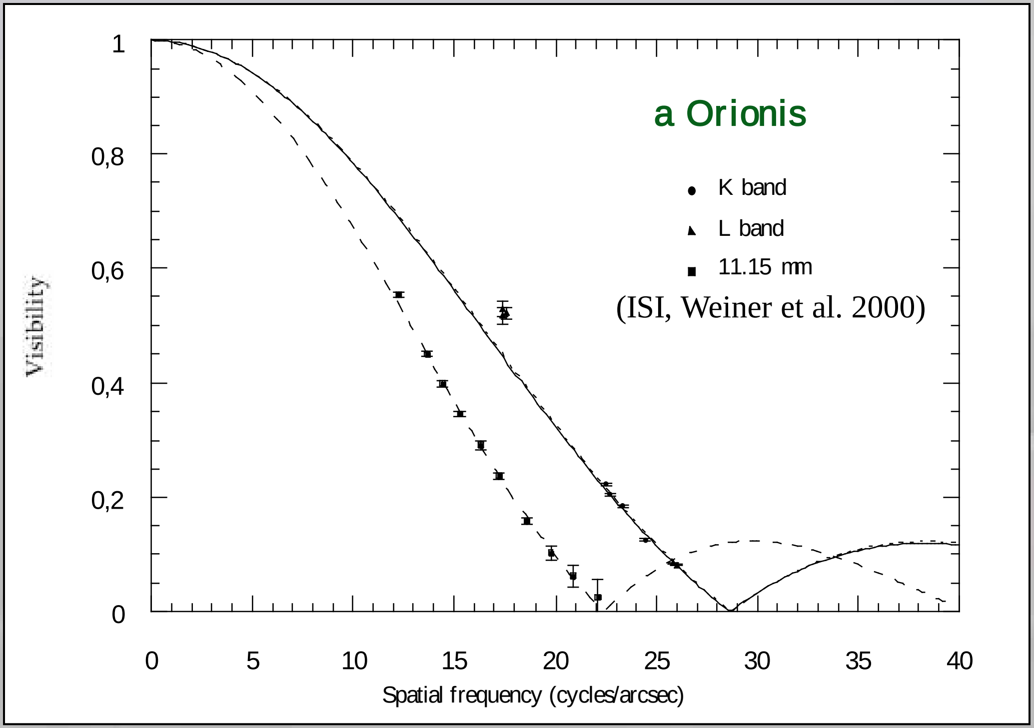

Perrin et al. (2004)

$$\varnothing_\star = 42.00 \pm 0.06\,\mathrm{mas}\,, \qquad T_\star = 3690 \pm 50\,\mathrm{K}$$
$$\varnothing_\mathrm{layer} = 55.78 \pm 0.04\,\mathrm{mas}\,, \qquad T_\mathrm{layer} = 2055 \pm 25\,\mathrm{K}$$
$$\tau_K = 0.060 \pm 0.003$$
$$\tau_L = 0.026 \pm 0.002$$
$$\tau_{11.15\mu m} = 2.33 \pm 0.23$$

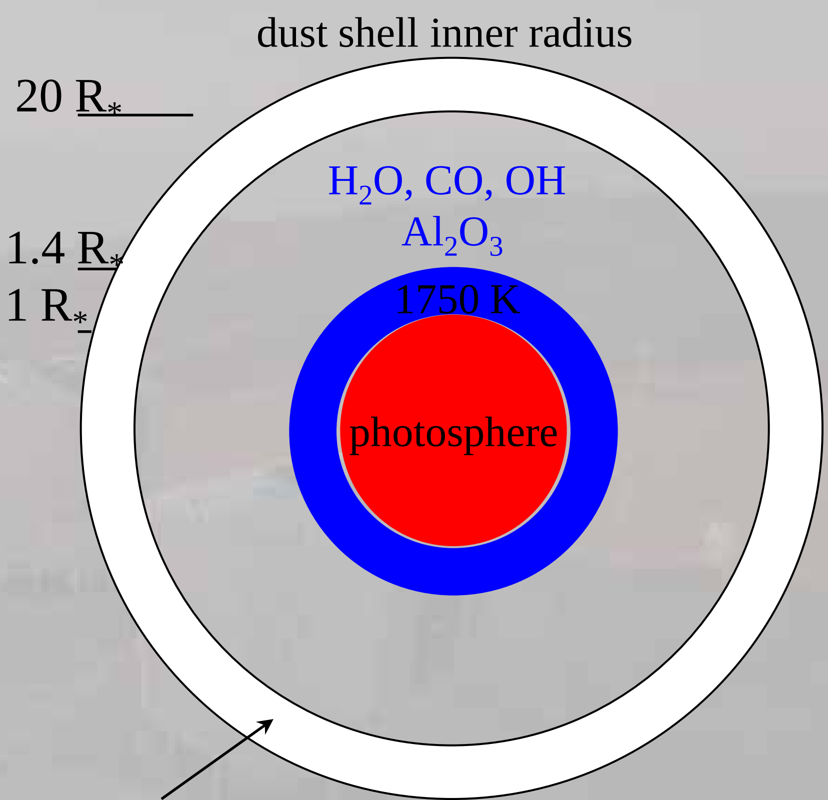

Danchi et al. (1994)

Ohnaka (2004)
Verhoelst et al. (2005)

Observations of Betelgeuse with MIDI

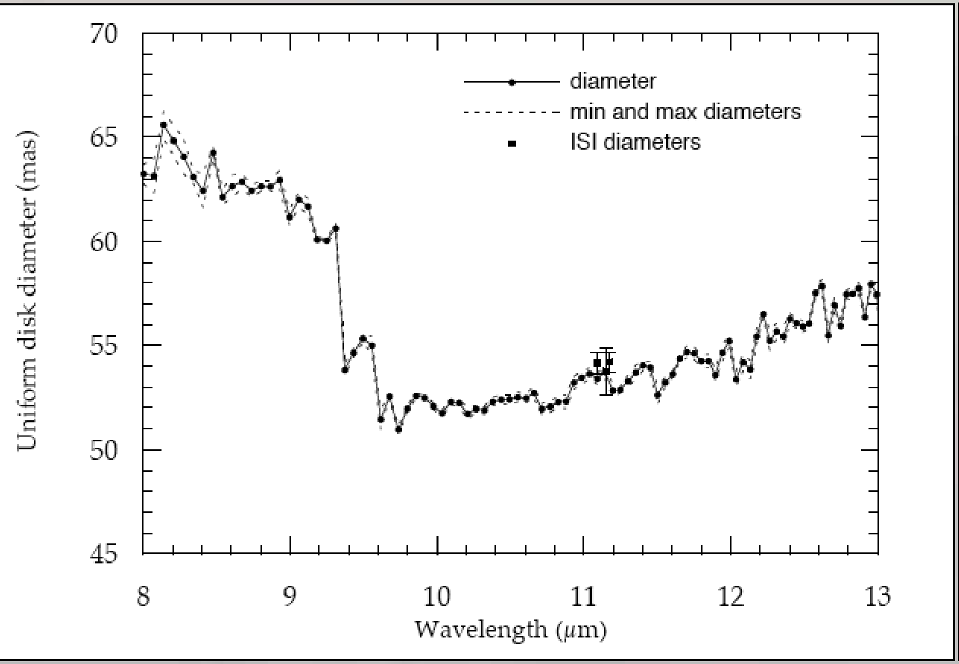

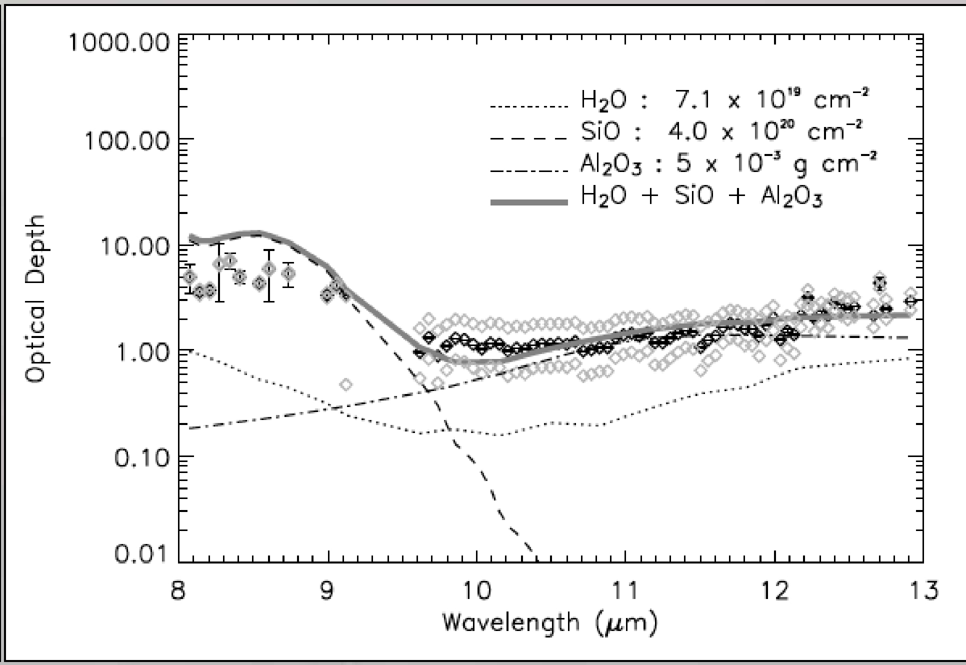

Perrin et al. (2007)

Observations of Betelgeuse with MIDI

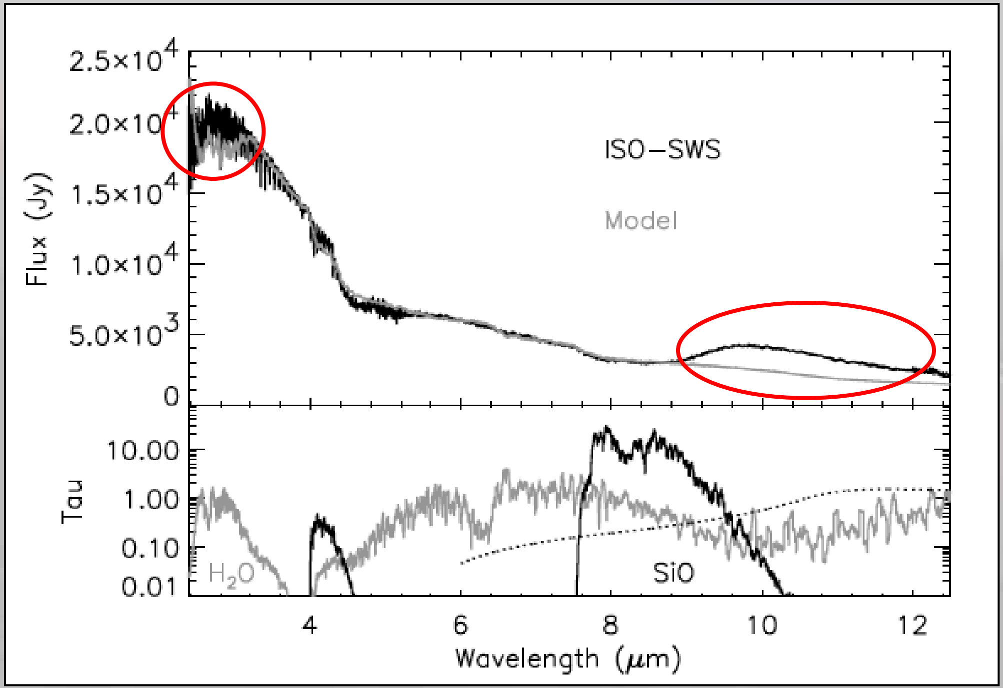

Component	N
H_2O [cm^{-2}]	$7.1 \pm 4.7 \times 10^{19}$
SiO [cm^{-2}]	$4.0 \pm 1.1 \times 10^{20}$
Al_2O_3 [g cm^{-2}]	$5.0 \pm 0.9 \times 10^{-3}$

Perrin et al. (2007)

Proposal for a scenario for dust formation:

- Al_2O_3 can condensate in the warm region of the MOLsphere (1700 K) where it is detected.
- SiO is adsorbed on Al_2O_3 grains in the MOLsphere and benefits from radiation pressure on solid grains.
- Silicate grains condensate at larger distance and cover Al_2O_3 grains which are no longer detected.

Issue to solve: lift the gas up to the MOLsphere without a steady pulsation regime.

The elusive diameter of Mira

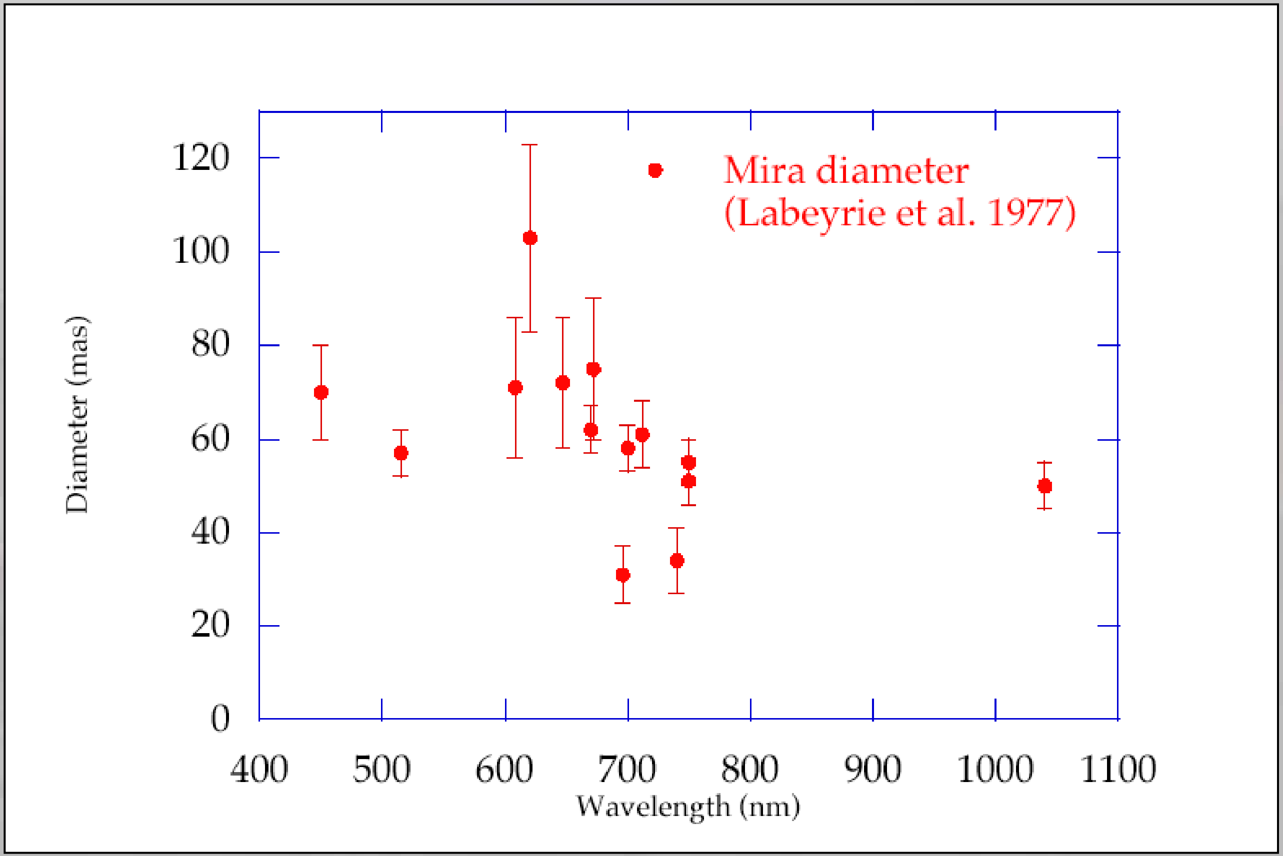

Observations in narrow bands in K

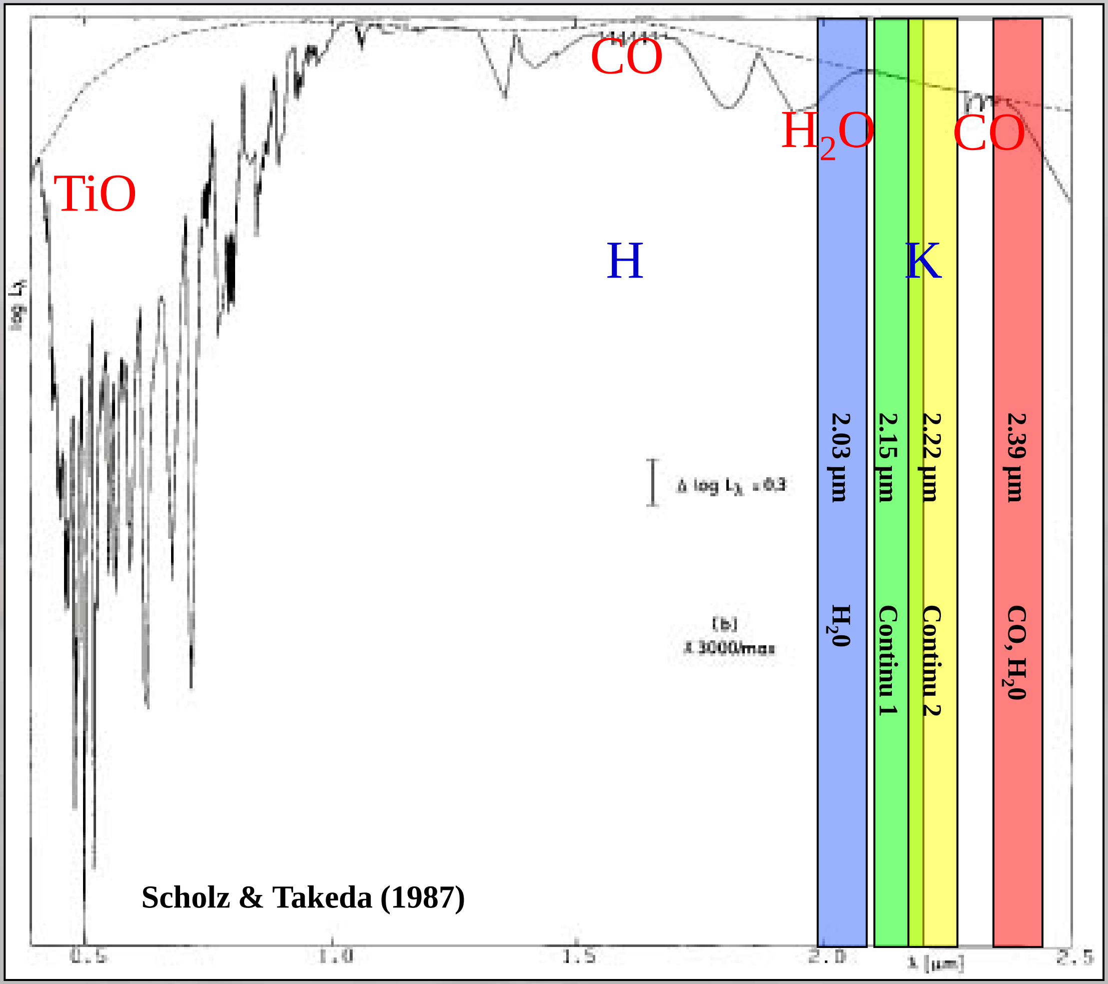

Simple ad-hoc model: photosphere + molecular shell

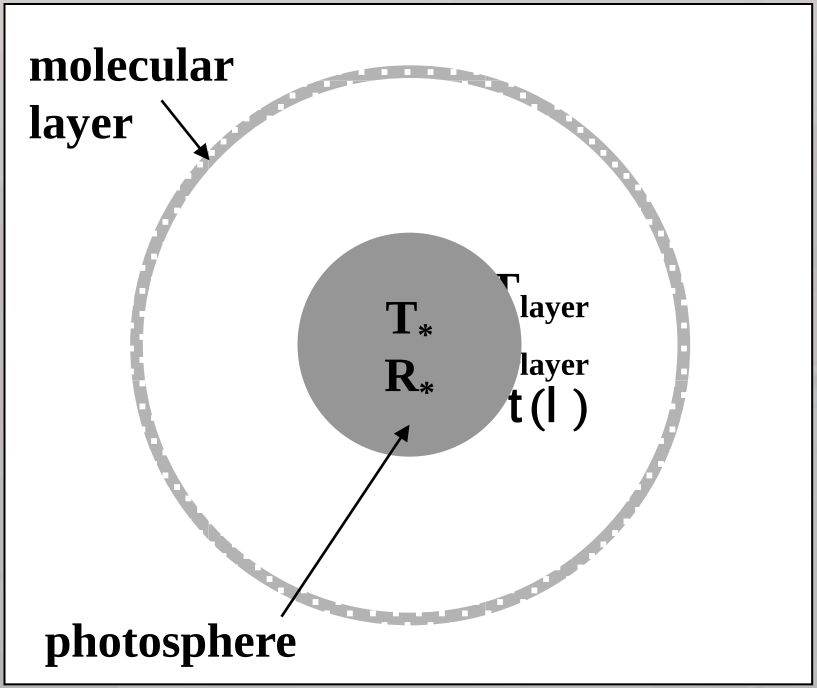

Perrin et al. (2004)

L band and K narrow bands

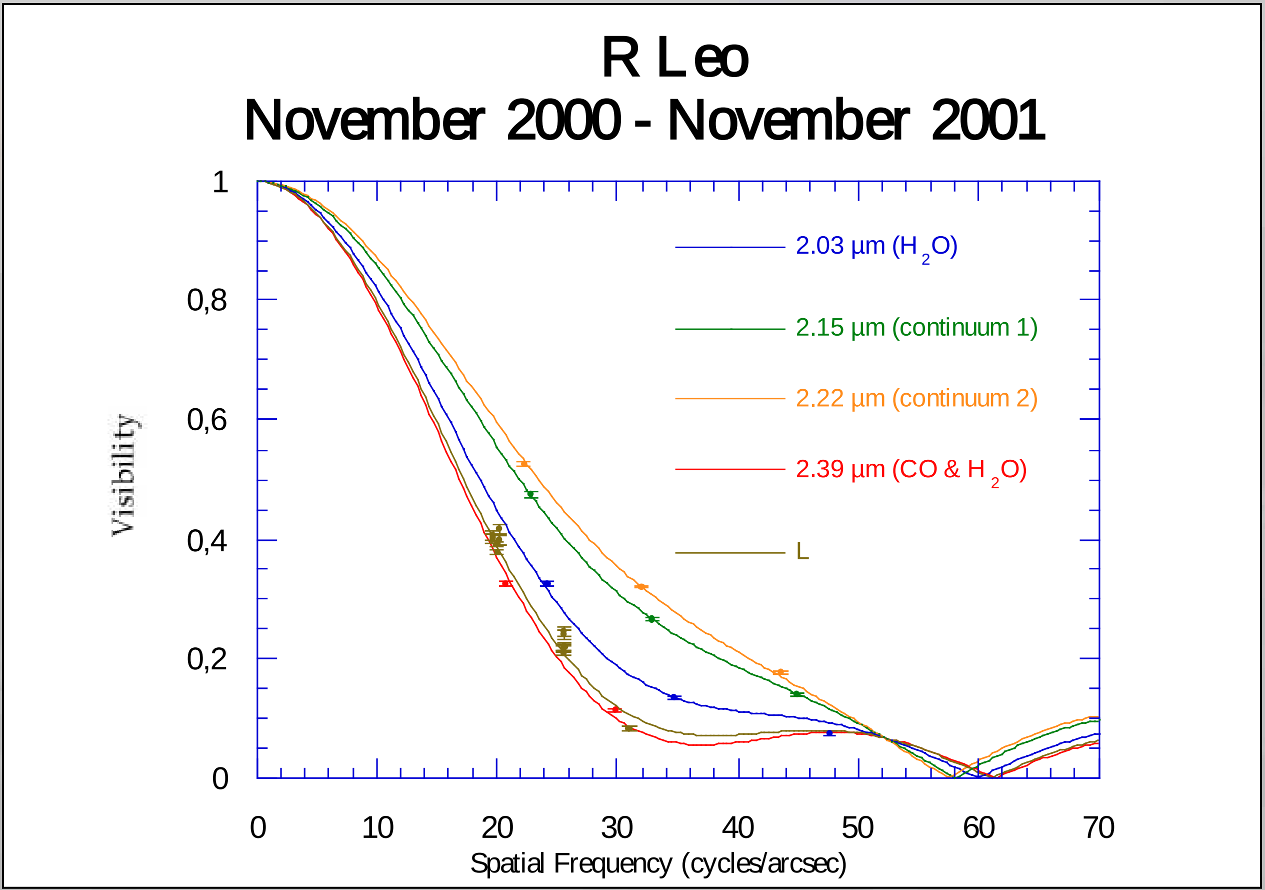

$t_{2.03\mu m} = 1.19 \pm 0.01$

$t_{2.15\mu m} = 0.51 \pm 0.01$

$t_{2.22\mu m} = 0.33 \pm 0.01$

$t_{2.39\mu m} = 1.37 \pm 0.01$

$t_{L} = 0.63 \pm 0.01$

$R_{layer}/R_{*} = 2.4$

Perrin et al. (2004)

R_{*} = 10.94±0.85 mas
T_{*} = 3856±119 K

R_{layer} = 25.00±0.17mas
T_{layer} = 1598±24 K

Phase K: 0.79
Phase L: 0.64

Type: M0-M1

R Vir at Keck

(Eisner et al. 2007)

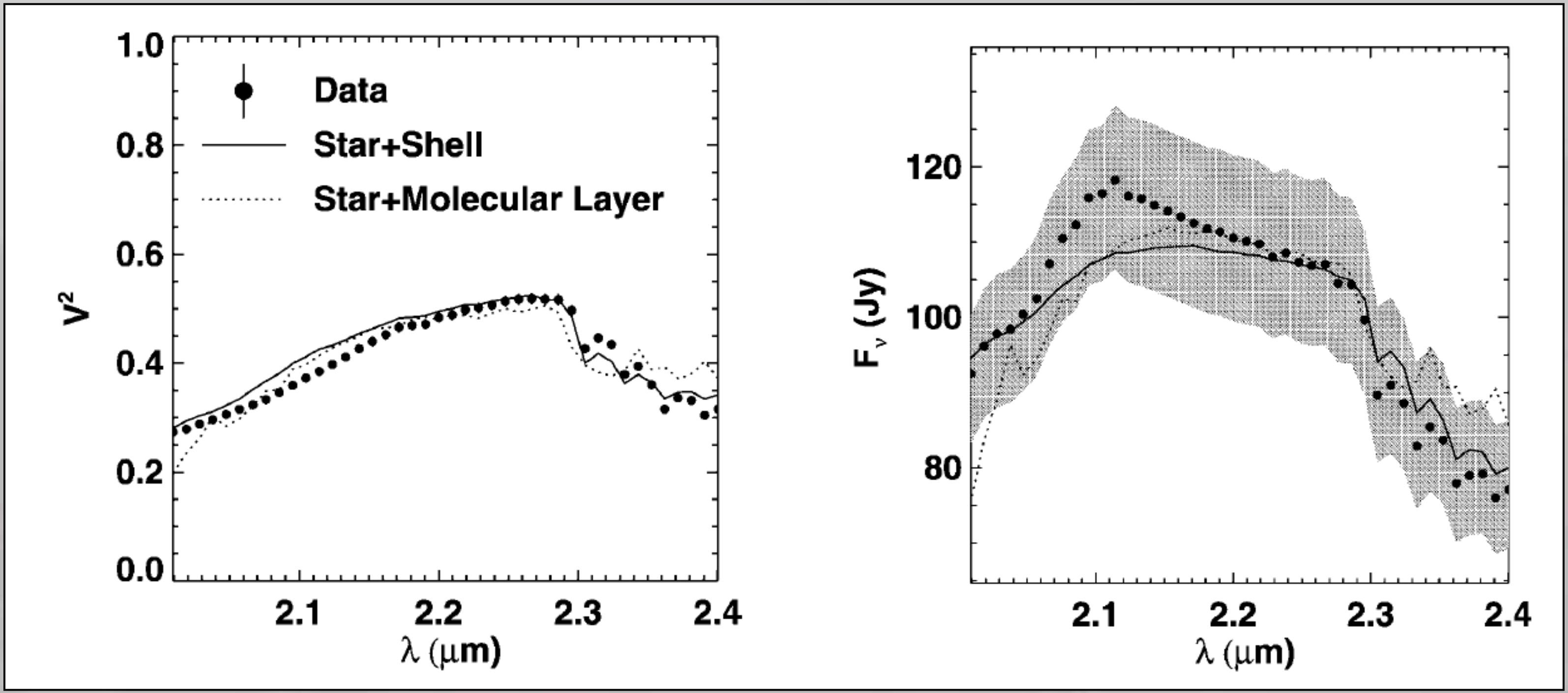

$T = 1800\,\mathrm{K}, N_{H_2O} = 5 \times 10^{20}\,\mathrm{cm}^{-2}$, and $N_{CO} = 10^{22}\,\mathrm{cm}^{-2}$

H_2O+CO layer

The contents of the molecular layer of RR Sco

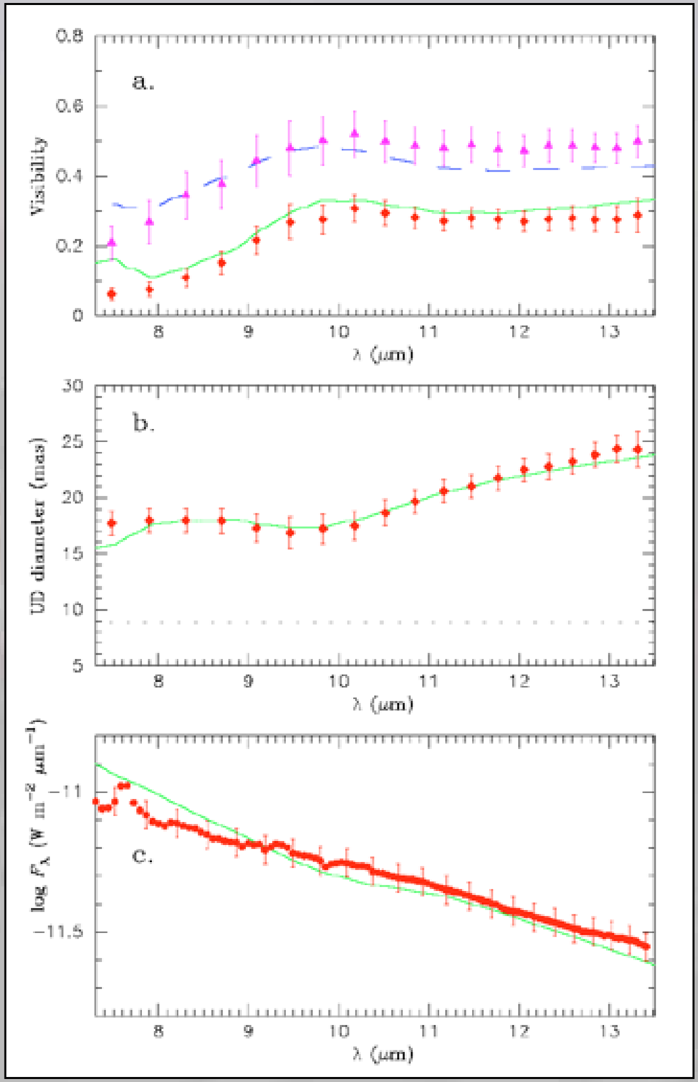

H_2O+SiO layer

T_{layer} = 1400 K
R_{layer} = 2.3 R_*

N_{H2O} = 3x10^{21} cm^{-2}
N_{SiO} = 1x10^{20} cm^{-2}

Ohnaka et al. (2005, MIDI)

General sketch for O-rich Mira stars

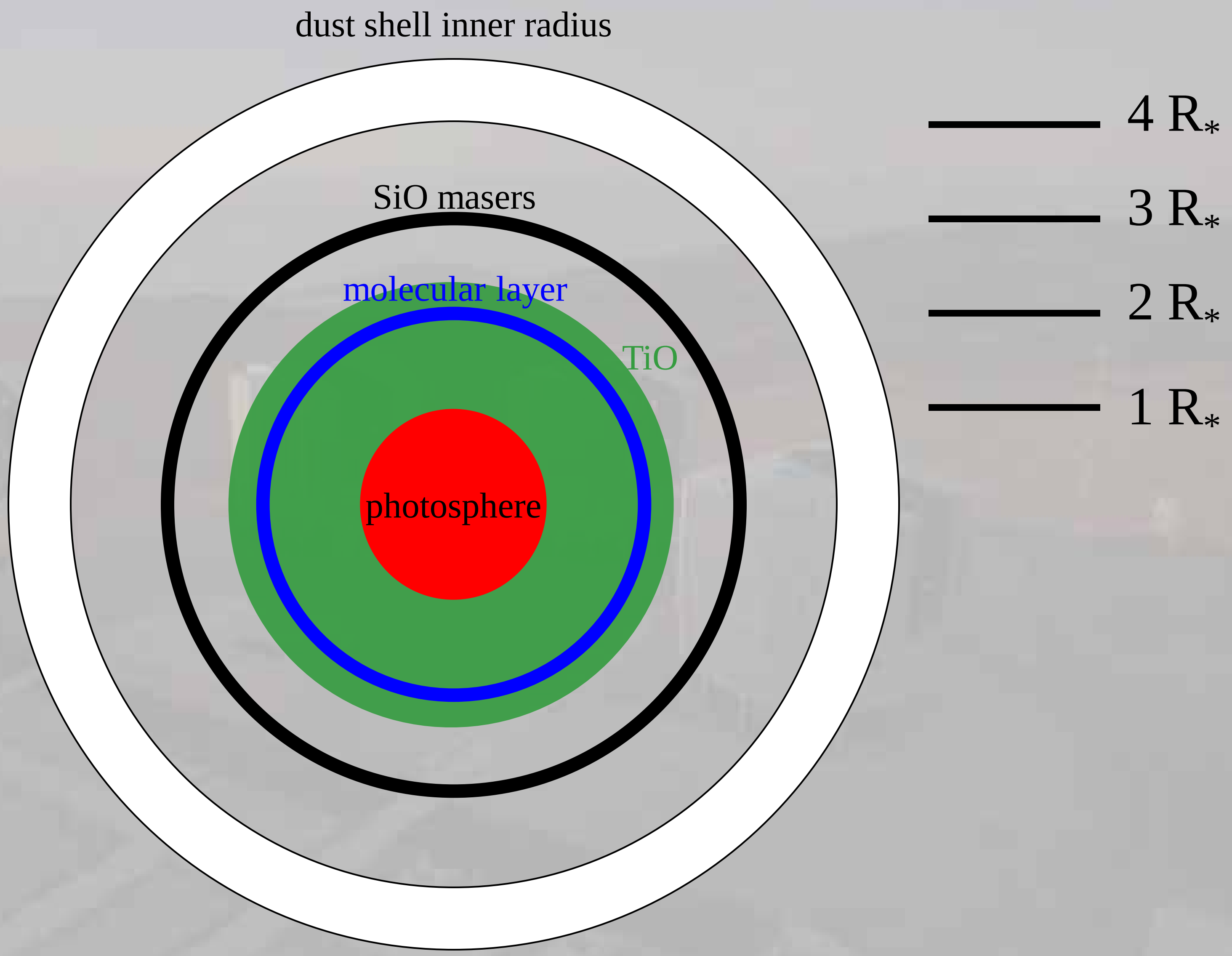

General sketch for O-rich Mira stars

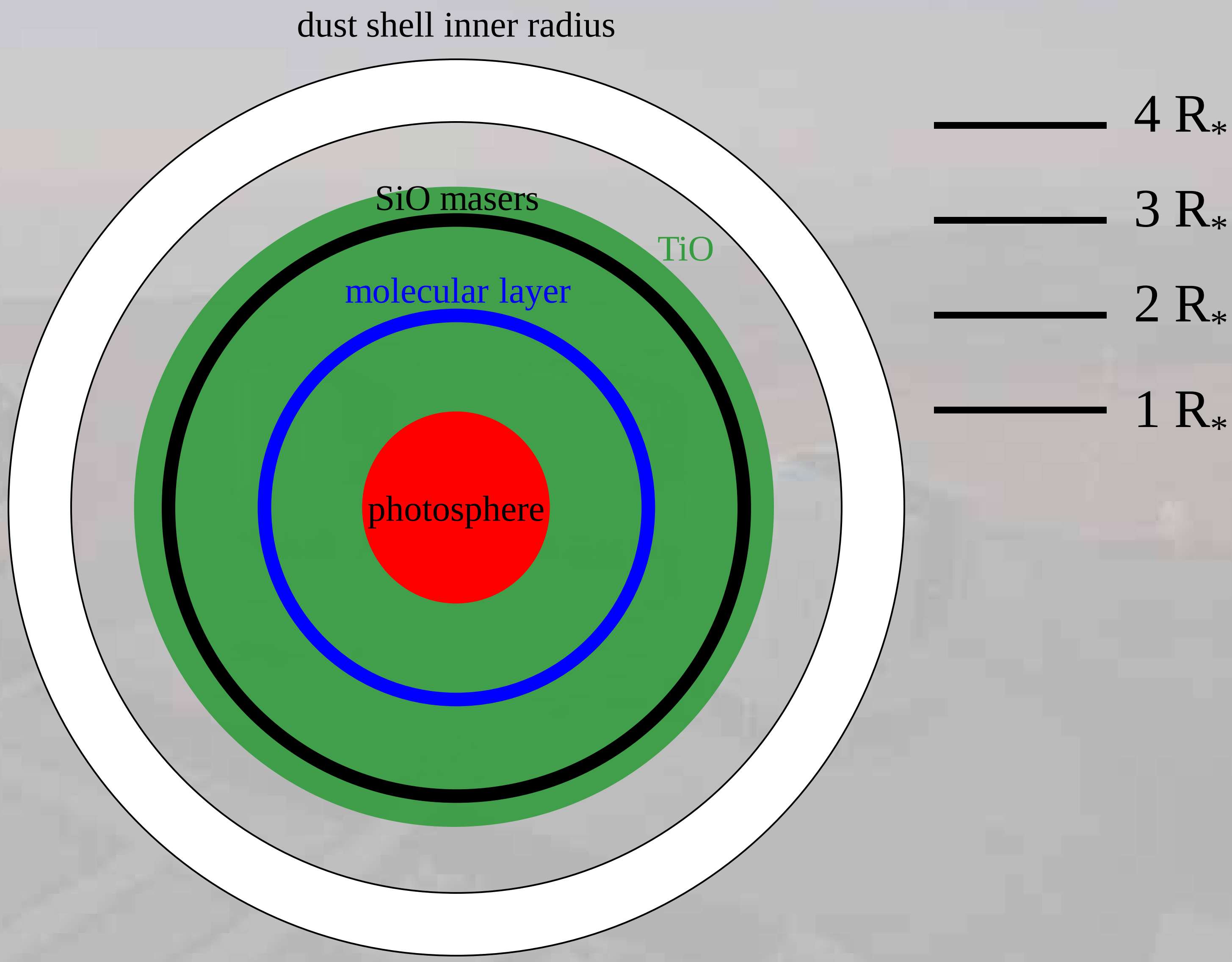

A new tool to study late-type stars: interferometric images

(u,v) coverage and image reconstruction

$$\frac{\vec{B}}{\lambda} = (u,v)$$

QuickTime™ and a decompressor are needed to see this picture.

Inverting the Zernike - van Cittert theorem is not an easy task in these conditions

$$V(\vec{B}) = \frac{\int_{source} I(\vec{S}) \exp\left[-2i\pi \vec{S}.\frac{\vec{B}}{\lambda}\right] d^2S}{\int_{source} I(\vec{S}) d^2S}$$

$$I(\vec{S})$$

Reconstructing images from a sparse (u,v) coverage

$$F = \frac{1}{N-p}\left(\sum_{V_i^2}\left(\frac{V_i^2 - M_V(S_i)}{\sigma_i}\right)^2 + \sum_{\text{closure phases}}\left(\frac{\varphi_i^{123} - M_\varphi\left(S_i^{123}\right)}{\sigma_i}\right)^2\right) + \text{regularization}$$

$$= \chi^2 + \mu\ \text{penalty function}$$

The penalty function is a regularization term which adds constraints to reconstruct the image (positivity, smoothness, limited extension, …)

The µ *hyper-parameter* can be adjusted to force the image to be mostly constrained by the *prior* or conversely to force the image to be mostly constrained by the data.

Mont Hopkins

Arizona

IOTA

Infrared and Optical Telescope Array

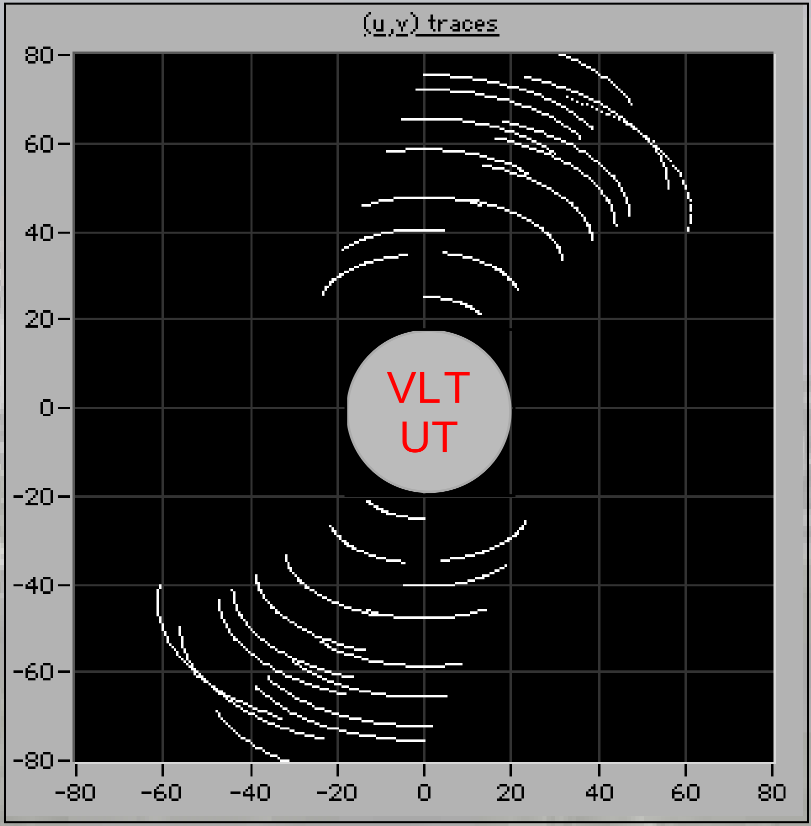

- 3 movable 45 cm siderostats
- Minimum baseline: 5m
- Maximum baseline: 38m
- Resolution in K band: 12 mas

- Passed away in July 2006 !

Arcturus at IOTA (H)

QuickTime™ and a
TIFF (Uncompressed) decompressor
are needed to see this picture.

Comparison of center-to-limb variations

parametric
WISARD
MIRA

QuickTime™ and a
TIFF (Uncompressed) decompressor
are needed to see this picture.

Lacour et al. (2008)

QuickTime™ and a
TIFF (Uncompressed) decompressor
are needed to see this picture.

T Lep at VLTI

Le Bouquin et al. (2009)

T Lep at VLTI

Le Bouquin et al. (2009)

Convective motions at the surface of Betelgeuse

(Ohnaka et al. 2009)

QuickTime™ and a
decompressor
are needed to see this picture.

Patchy
surface
model

Date of observation: January 2008

Large upwelling spot (≤ hemisphere, Q=60°)
10-15 km/s velocity

Detected in the blue and red wings of CO lines in K band with AMBER.

Imaging the surface of Betelgeuse with IOTA in the H band (Haubois et al. A&A 508, 923, 2009)

October 2005 observations

MIRA algorithm

WISARD algorithm

PSF

Assuming blackbody emission for spot T_1:

$T_* = 3600$ K
$T_{spot} = 4125$ K

It is compatible in size (~ 10 mas) and temperature with a convective cell.
T_2 is unresolved and is close to the pole.

Location of the polar cap from HST imaging Uitenbroek et al. (1998)

Comparison of the Betelgeuse H band data with convection models (Chiavassa et al., submitted to A&A)

Hydrodynamical simulations of convection (CO^{5}BOLD+OPTIM3D)

Comparison to V^2

Comparison of the Betelgeuse H band data with convection models (Chiavassa et al., submitted to A&A)

Hydrodynamical
model of convection

Comparison to closure phases

Large plumes with NACO (Kervella et al., 2009, A&A **504**, 115)

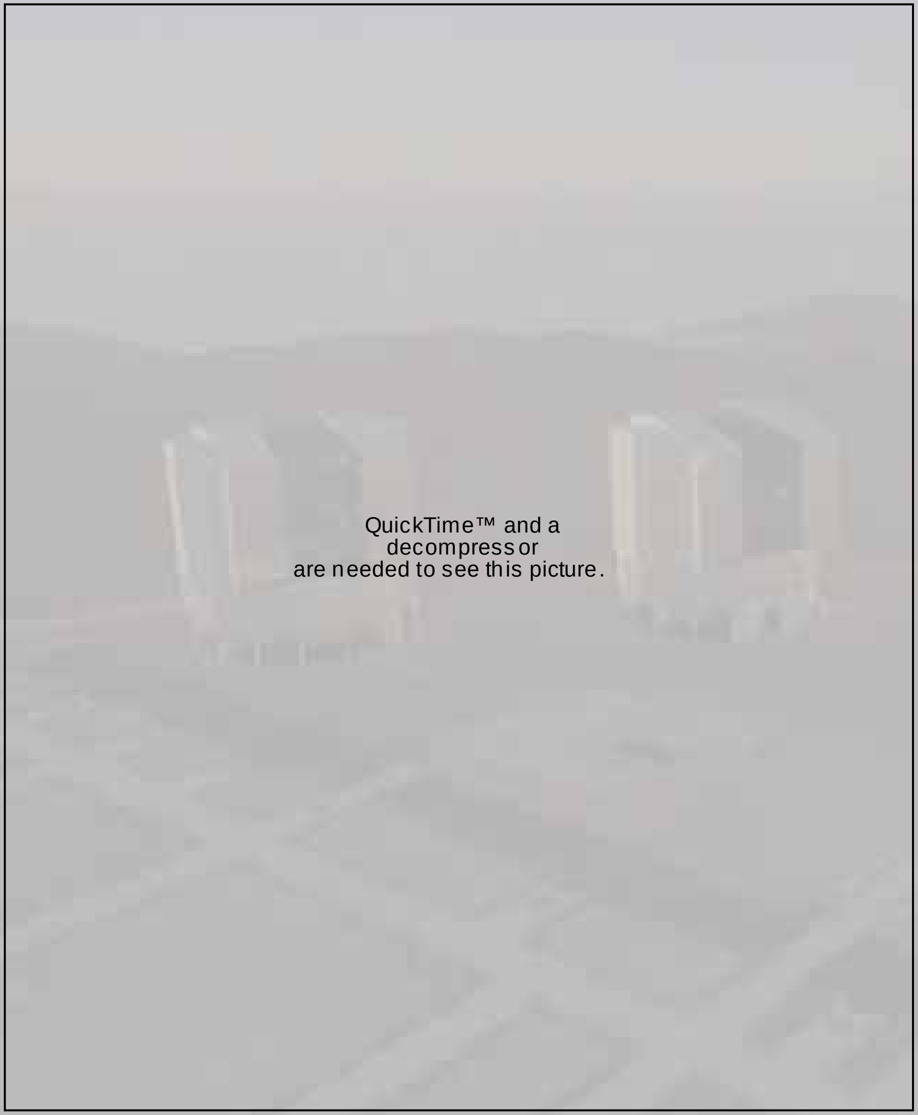

JHK NACO images in burst mode (January 2009)

The asymmetric close environment (6R*) may be explained by mass-loss triggered by convection.

CN is detected in absorption in the environment.

The Southwestern plume may be linked to either convection or to stellar rotation.

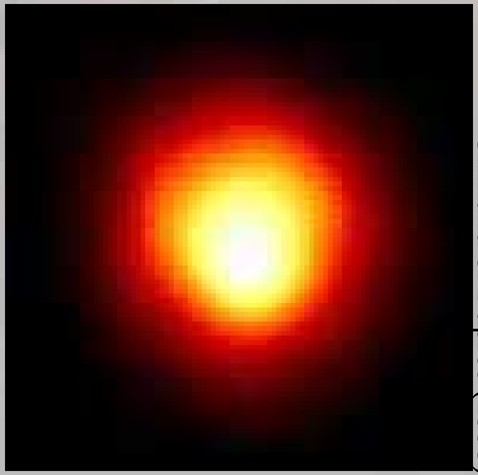

Gilliland & Dupree (1995)

1994 HST UV image

Detection of a magnetic field with NARVAL (Pic du Midi)

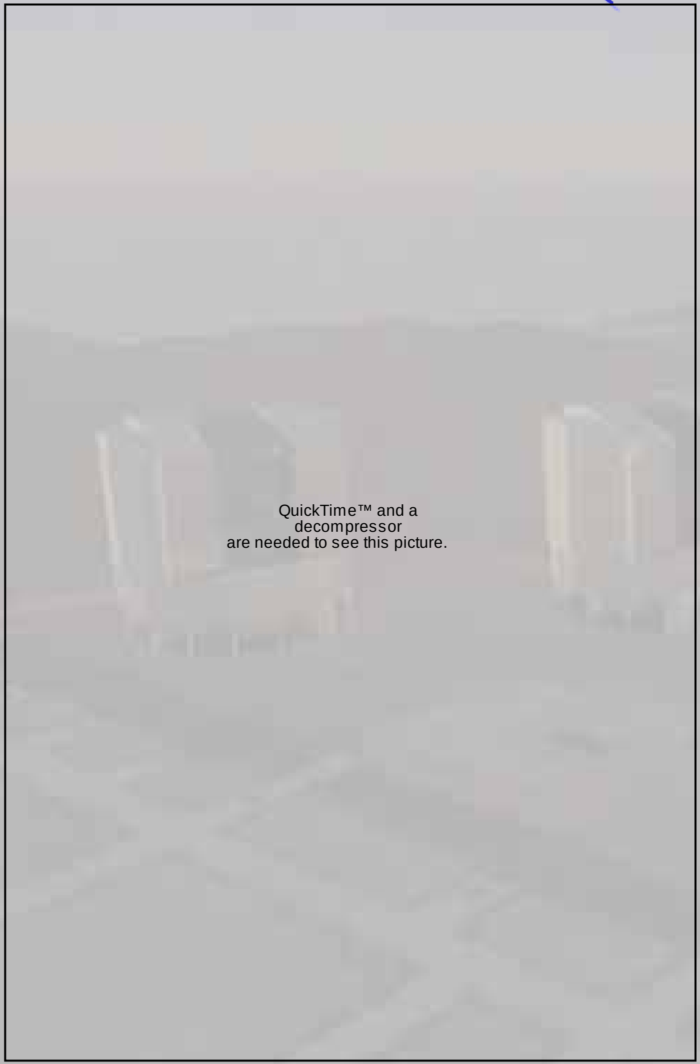

(Aurière et al., 2010, submitted to A&A L)

Detection of magnetic field on Betelgeuse (Zeeman splitting of lines).

Average magnetic field over the star surface:

$$0.5\ \mathrm{G} \leq B \leq 1.5$$

Possibly of convective origin -> follow the evolution of the magnetic field.

Conclusions for Betelgeuse

- Evidences of direct detection of convection at the surface of the star.
- Convection cells may be connected with plumes imaged up to a few stellar radii that contain at least one molecule, CN.
- There is a consistent scenario to explain dust formation and mass loss thanks to the detection of the MOLsphere.
- Convection is a strong candidate to provide energy to levitate gas up to the MOLsphere. The detection of a magnetic field is a hint that this phenomenon may play a role.

Are we touching the goal?

Mira in H band (Perrin et al., in preparation)

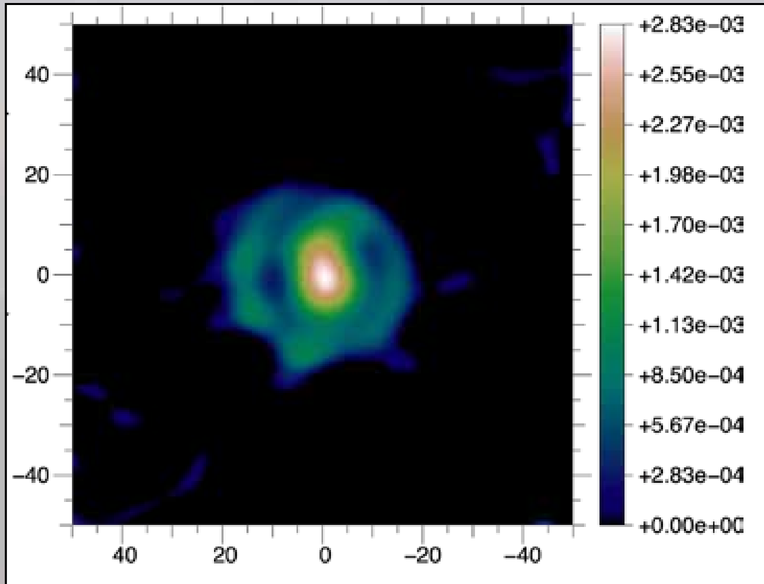

Image in the H band (IOTA)

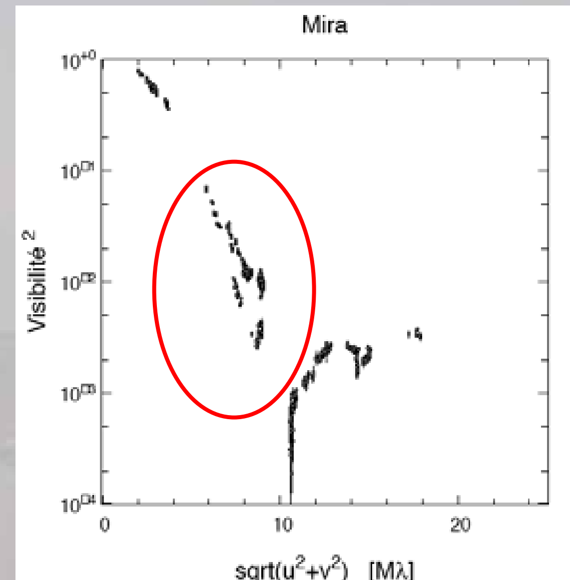

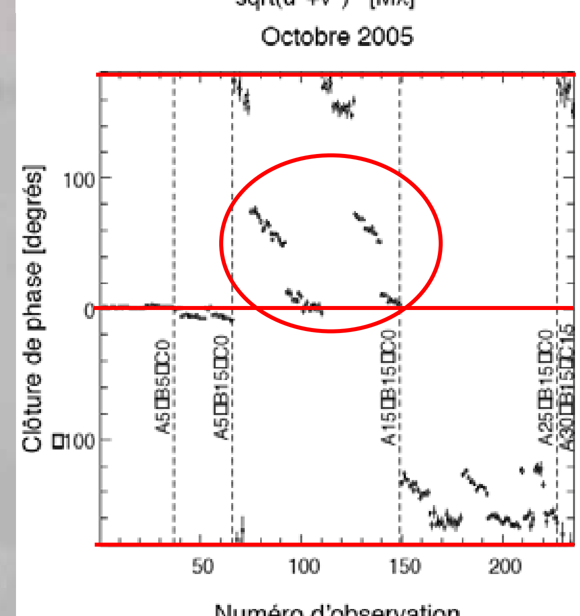

Mira in H band (Perrin et al., in preparation)

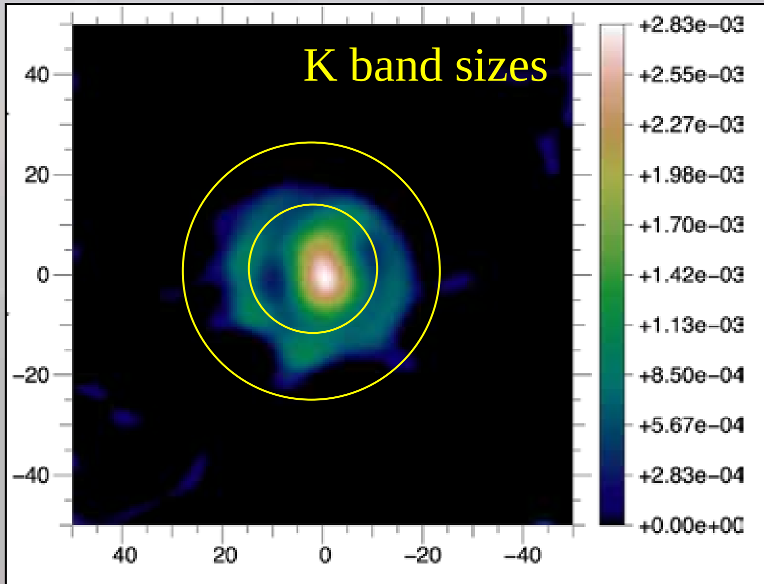

Image in the H band (IOTA)

QuickTime™ and a
decompressor
are needed to see this picture.

Perrin et al. (2004)

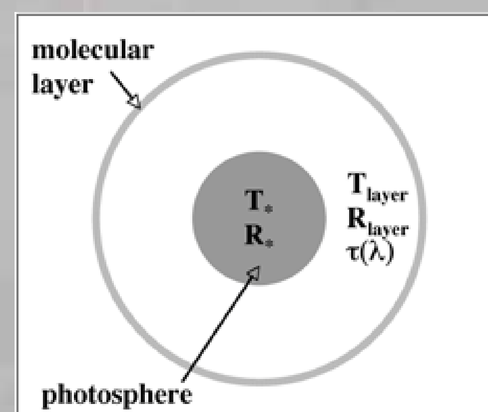

Point Spread Function

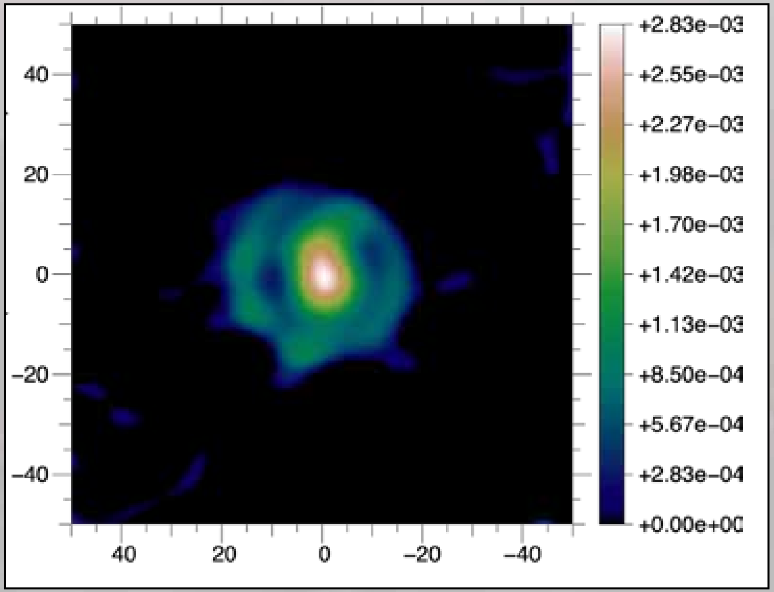

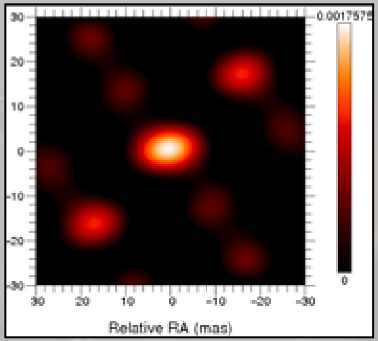

9x12 mas PSF

Comparison to the star + shell model

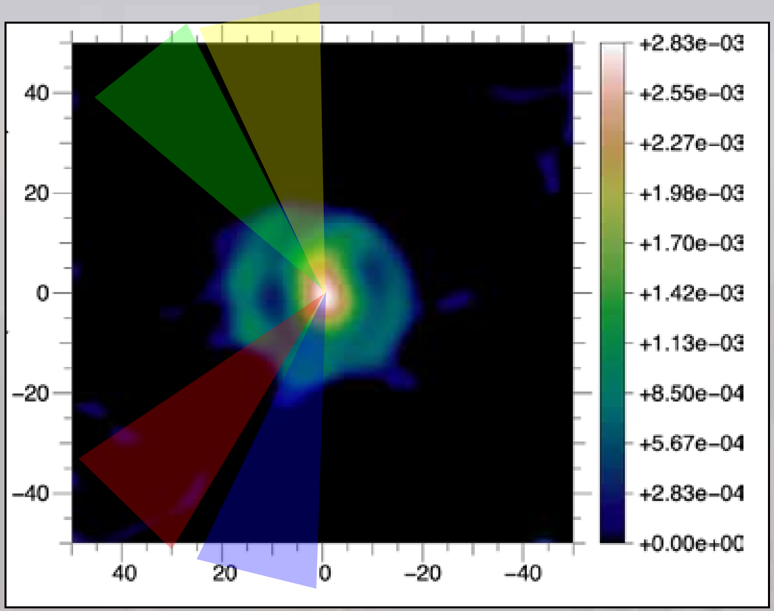

Baseline orientation

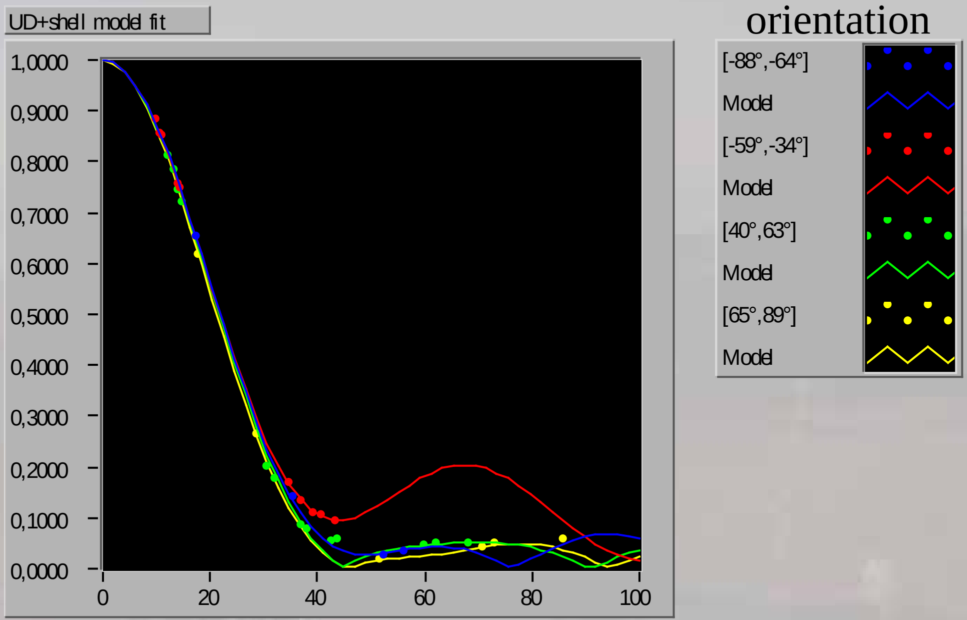

T_* = 3400 K
T_{shell} = 2000 K

[-88°,-64°]	[-59°,-34°]	[40°,63°]	[65°,89°]
D_* = 19 mas	D_* = 10 mas	D_* = 26 mas	D_* = 25 mas
D_{shell} = 39 mas	D_{shell} = 37 mas	D_{shell} = 43 mas	D_{shell} = 42 mas
t = 0.96	t = 0.44	t = 0.49	t = 0.65

Mira bi-polar outflow

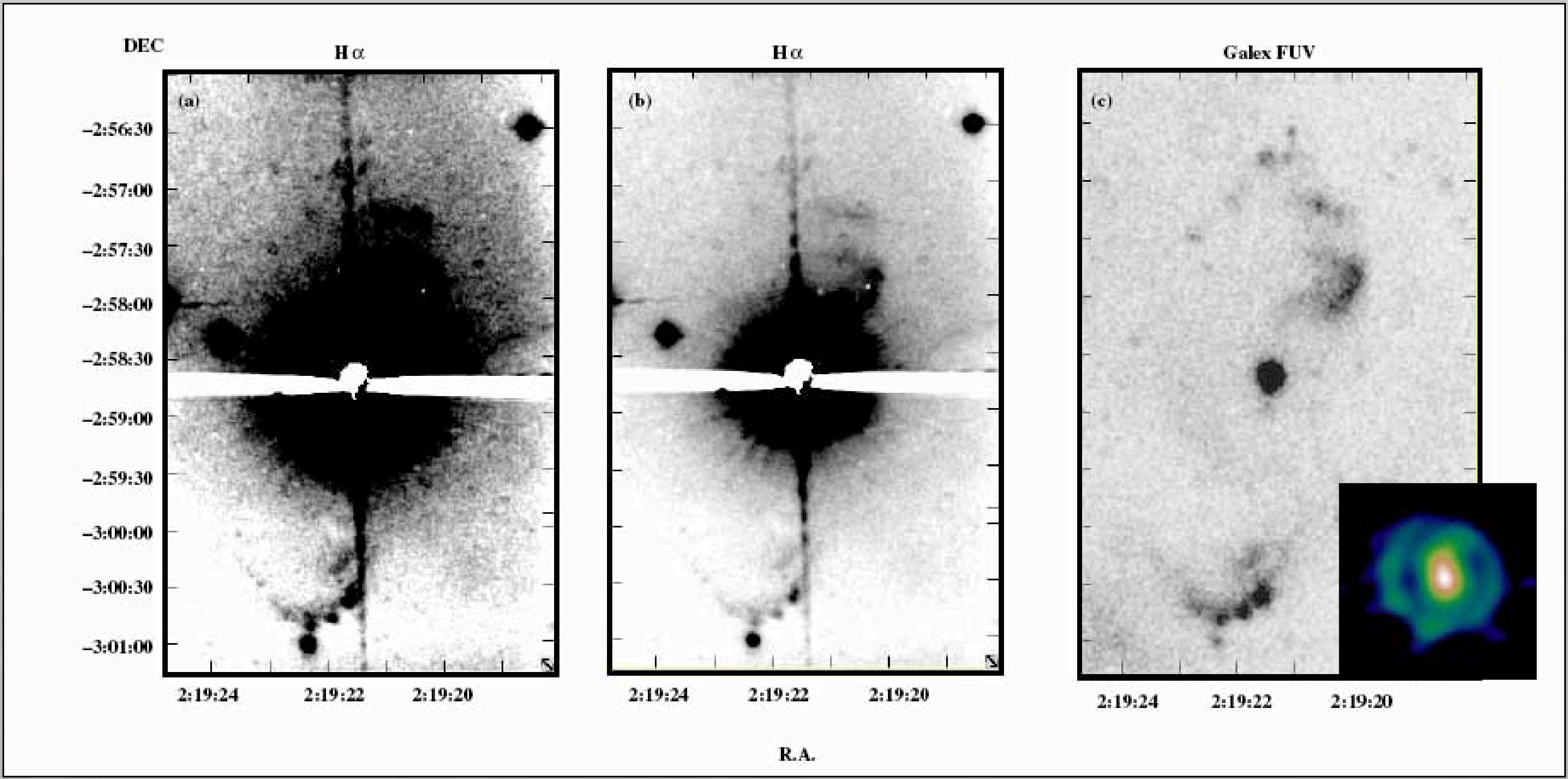

(Meaburn et al., 2009, A&A **500**, 827)

Average profile

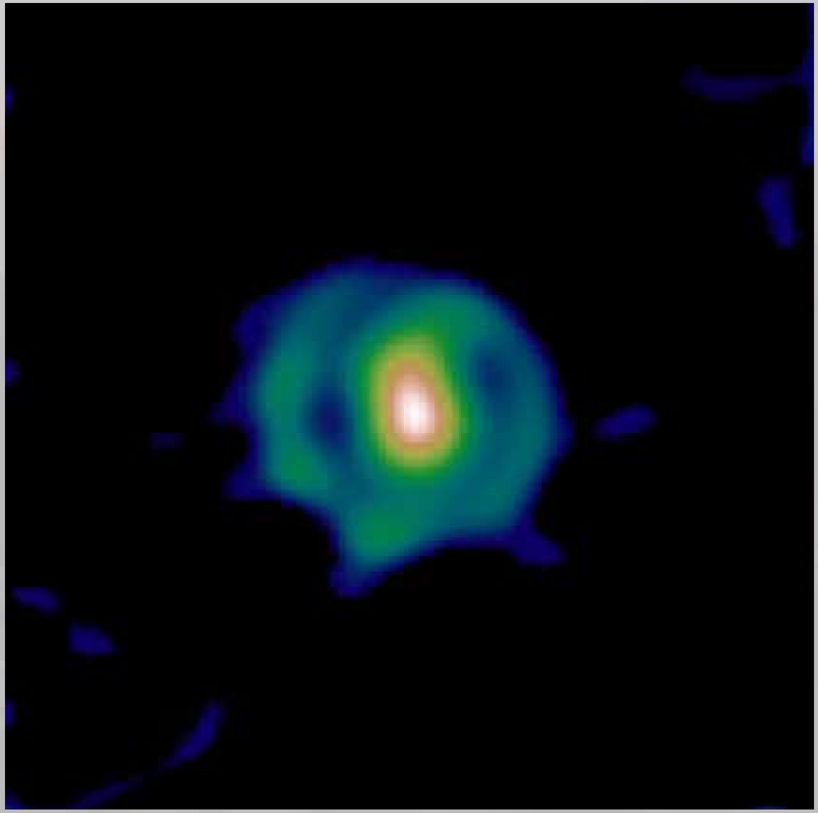

Original image

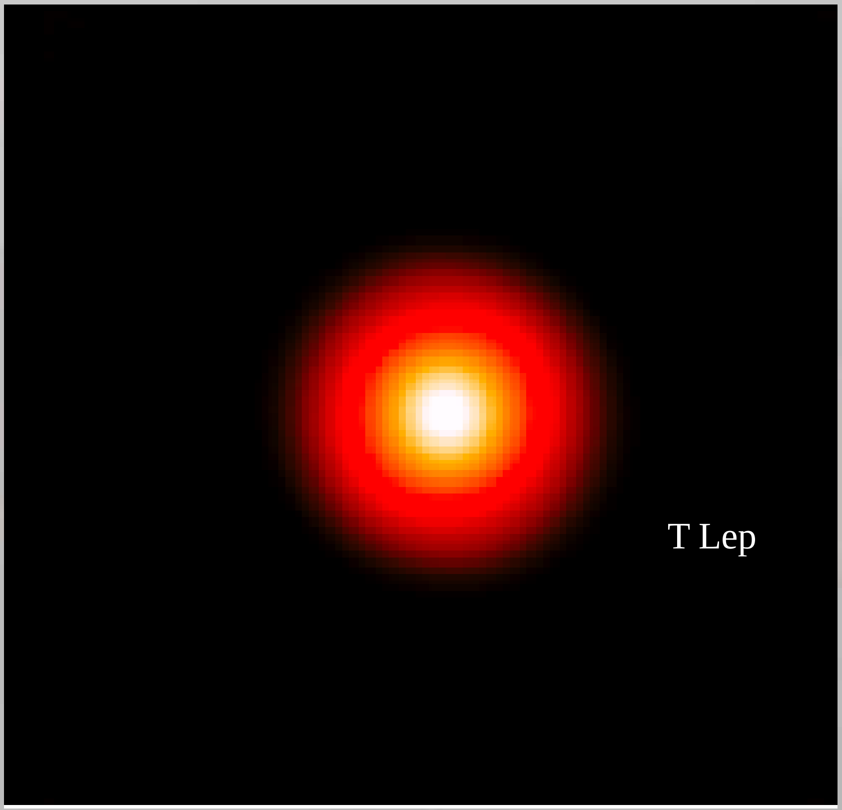

Azimuthally averaged image

Subtracting the average radial profile

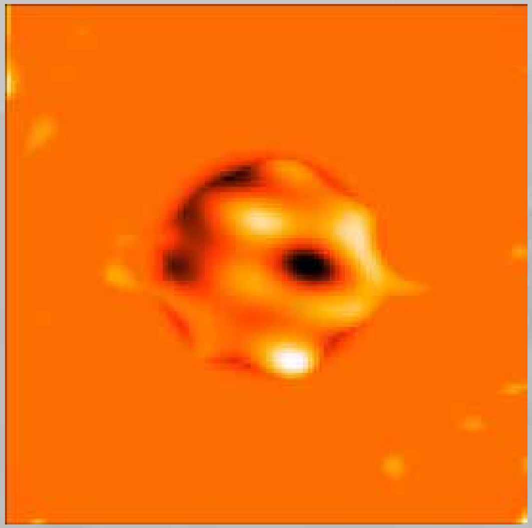

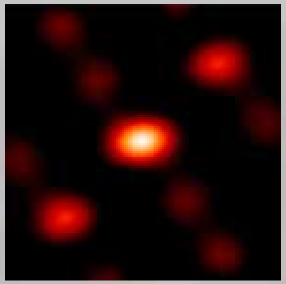

Convection

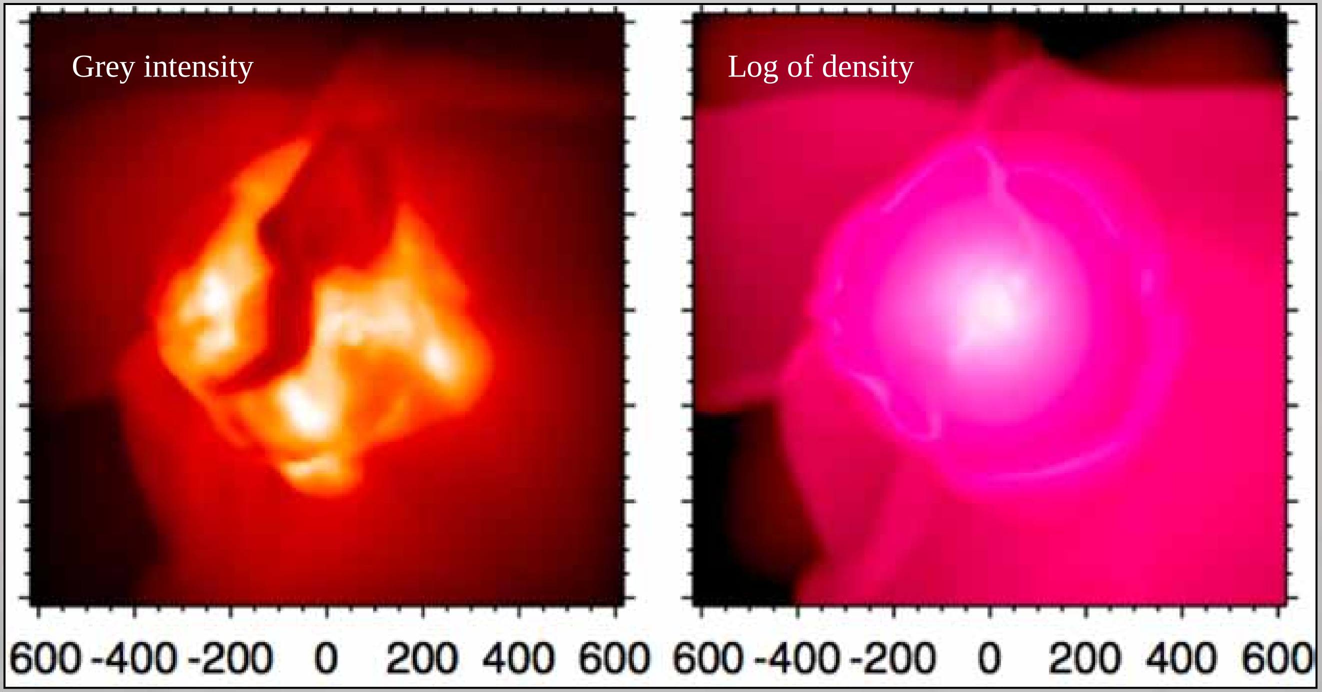

(Freytag & Höfner, 2008, A&A **483**, 571)

Snapshot of a hydrodynamical model of an AGB star incorporating both convection and pulsation.

Looking for the hidden behind the scene

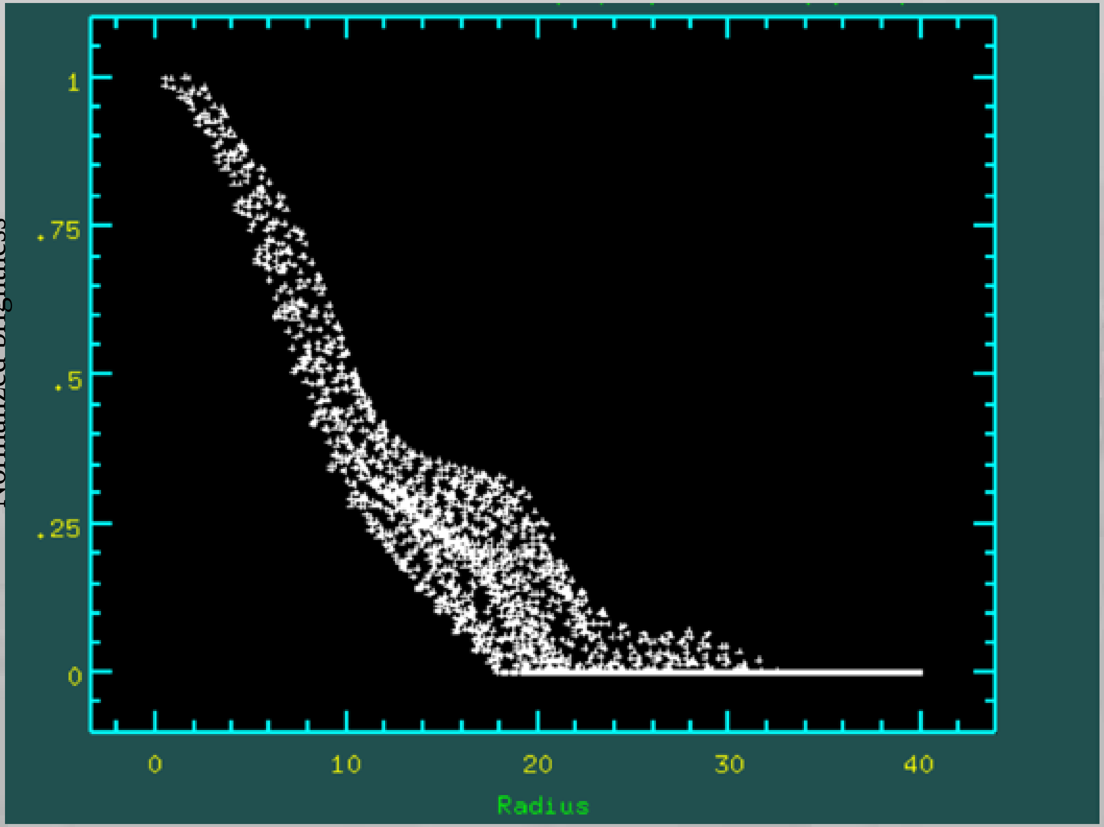

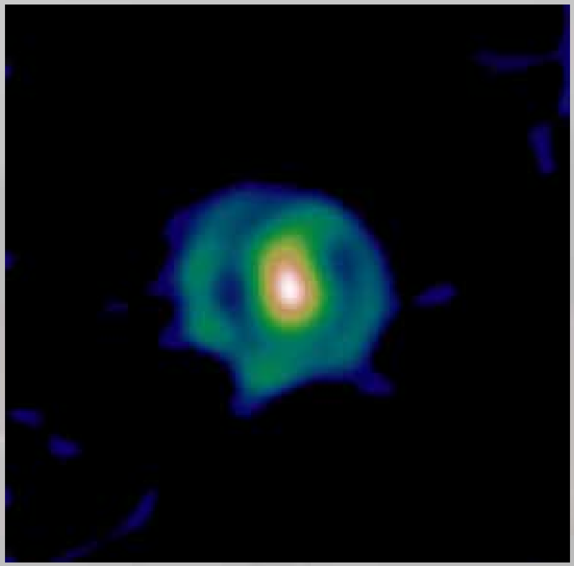

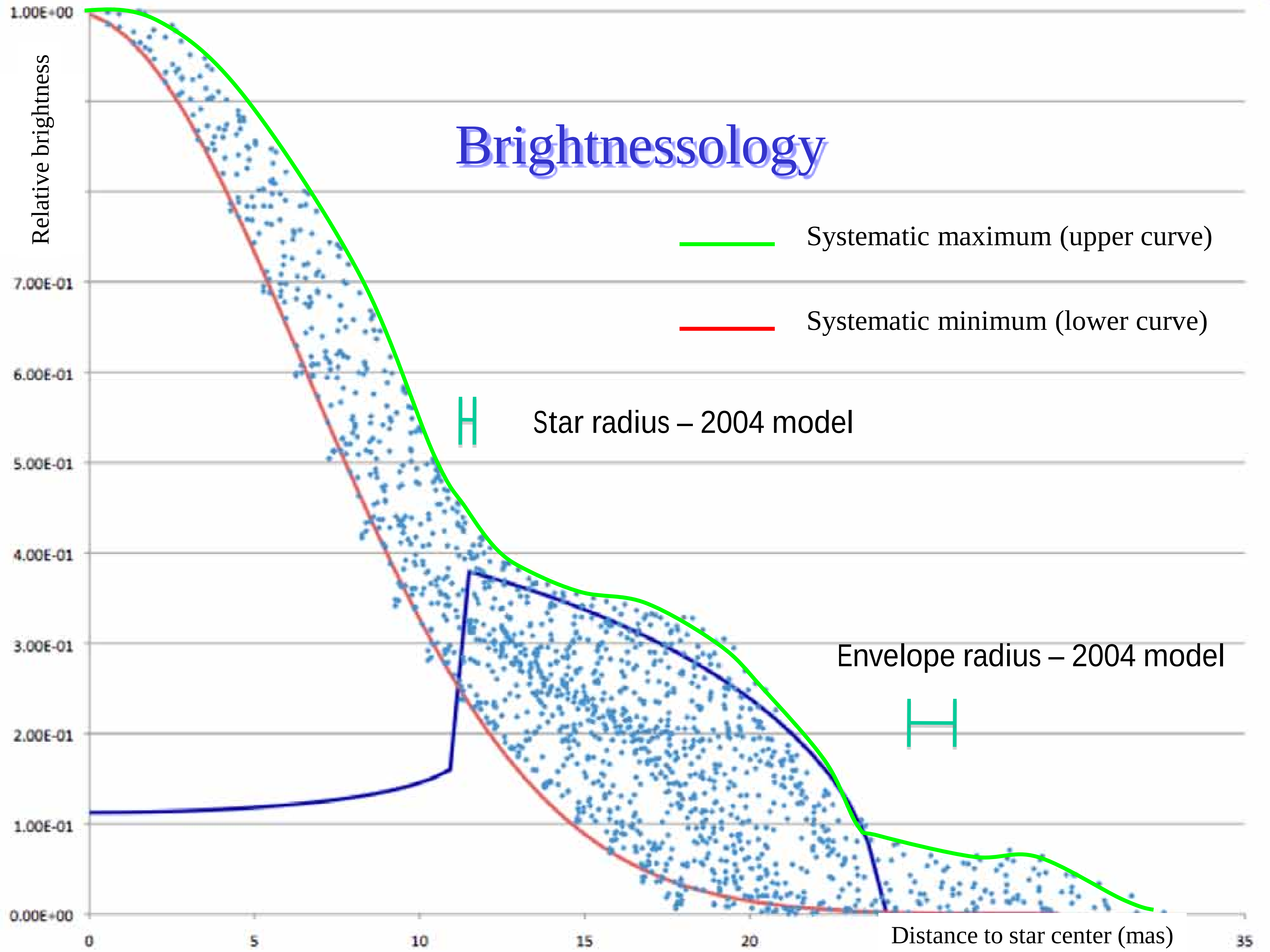
Brightnessology
Relative brightness
Systematic maximum (upper curve)
Systematic minimum (lower curve)
Star radius – 2004 model
Envelope radius – 2004 model
Distance to star center (mas)
1.00E+00
7.00E-01
6.00E-01
5.00E-01
4.00E-01
3.00E-01
2.00E-01
1.00E-01
0.00E+00
0
5
10
15
20
35

Tentative ideas

The Mira envelope contains regions of high density, making dark spots, which are as important or more important to the image structure than “bright” spots.

The radial brightness profiles show the size of the star and envelope, and the density of the envelope.

The gaussian profile may be the minimum profile when the star is fully covered by dark spots whereas the maximum profile is for an unspotty star.

The high density spots may be connected to nucleation sites for dust.

Dust shells around Mira

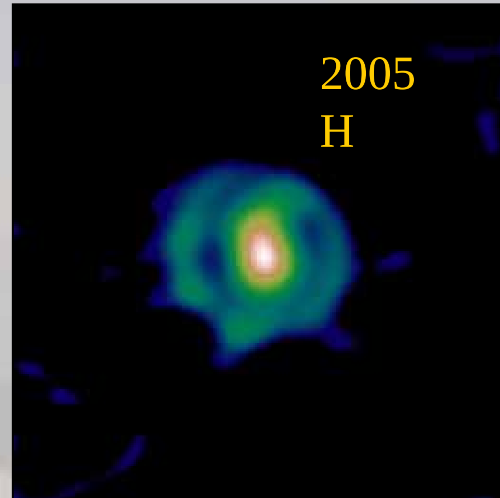

ISI 11.15 μm imaging data (Chandler et al. 2007)

2003

QuickTime™ and a decompressor are needed to see this picture.

5R* 20R*

2004 2005

QuickTime™ and a decompressor are needed to see this picture.

Shells are created and propagate outwards

Creation rate is not necessarily correlated to stellar pulsation Monnier et al. (2000, ISI)

Fluctuations of star maximum

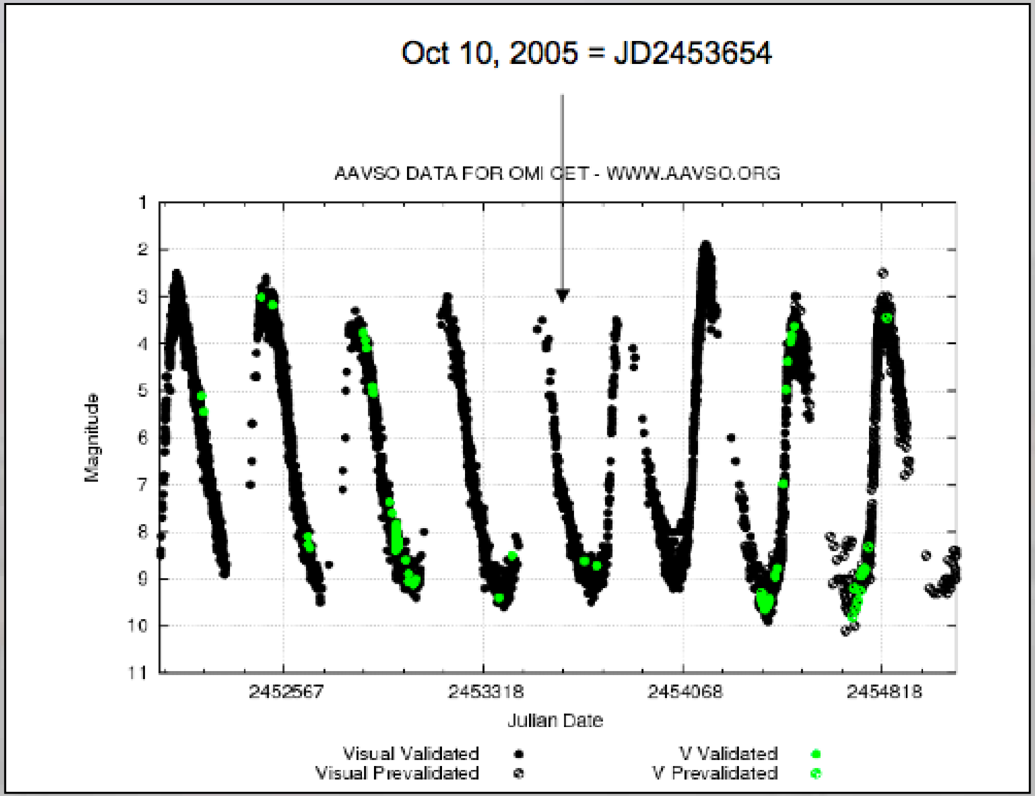

Could the amplitude of maxima be correlated with the number of dark spots ?

Ideas to study

Dark spots could be the result of convective uplift of material.

The variation in the number of dark spots could explain the cycle-to-cycle variation in the maximum brightness.

The North-South elongation of the Mira brightness could be associated with the bipolar outflow.

Could there be priviledged locations of spots because of magnetic fields that could induce a steady elongation ?

Dark regions could be areas of dust formation and produce asymmetric mass loss.

Conclusions

Conclusions (1/2)

- **Molecular environments are measured (MOLsphere)**
  - Gaseous reservoir at 2-2.5 R_* for Miras
    at ~ 1.4 R_* for red supergiants
  - List of constituents: TiO (visible), CO, H_2O, OH, Al_2O_3, SiO

- **A scenario has been proposed for dust formation in supergiants that may apply to Mira stars:**
  - Condensation of alumina in the molecular shell first with adsorption of SiO;
  - Silicate dust forms when temperature drops below 1000 K.

- **Convection may bring the missing momentum to lift up material in the atmosphere of red supergiants**

Conclusions (2/2)

- **Fundamental mode** pulsation cannot produce asymmetries.
- Asymmetries are a possible signature of **convection** (an alternative to binarity)
- **Convective cells** have been detected at the surface of **Betelgeuse** and the detected **plumes** may have a convective origin (building of the MOLsphere).
- Convective features possibly detected at the surface of c Cyg (shallow shell) and Mira (thicker shell).
- The asymmetry of Mira is interpreted to be the cause of a locally high density in the MOLsphere.

Interferometric imaging is beginning to help a lot

Origin of the spot brightness

Thermal emission from spot

Stellar radiation transmitted through spot

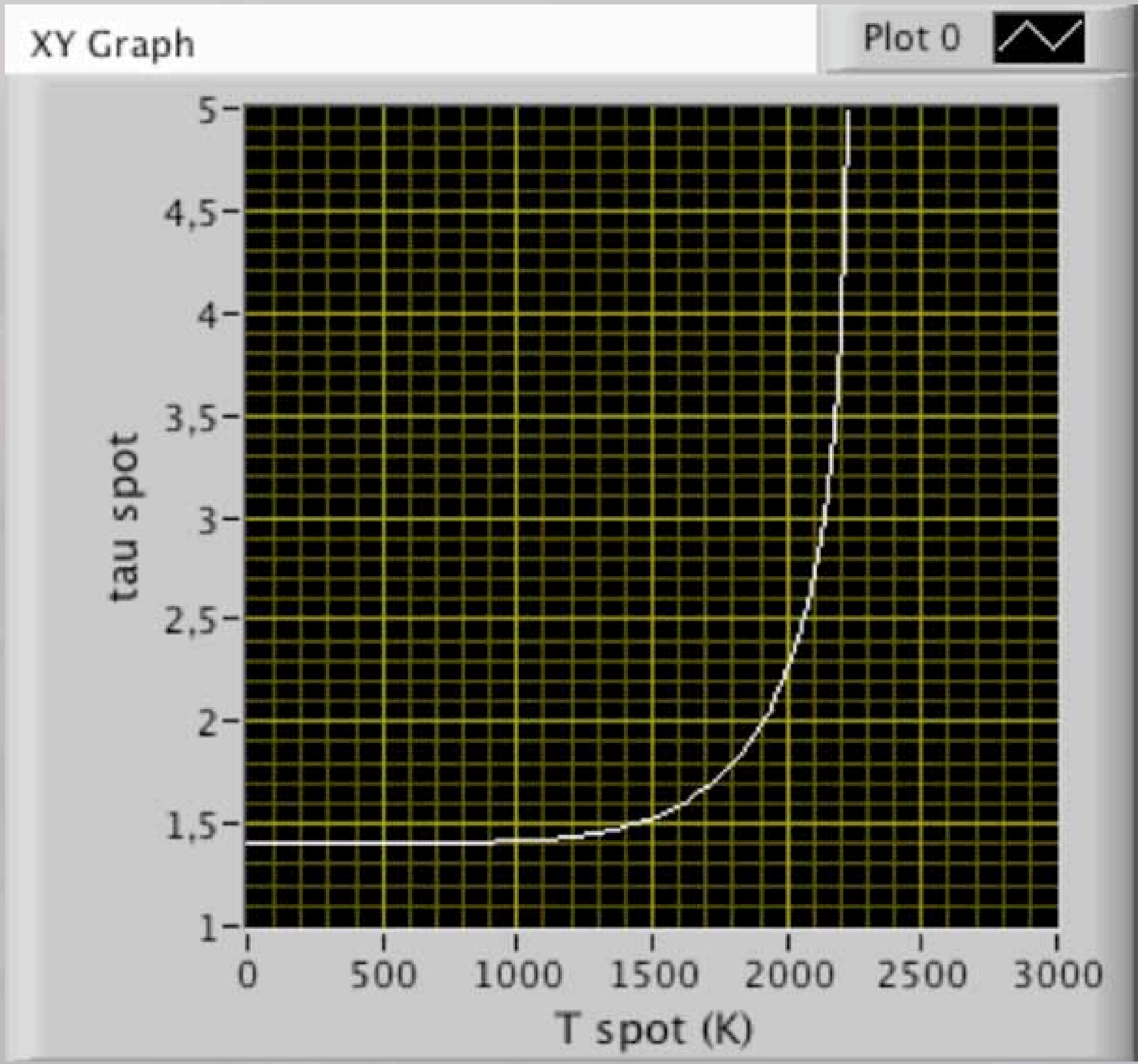

Could the companion provide an explanation ?

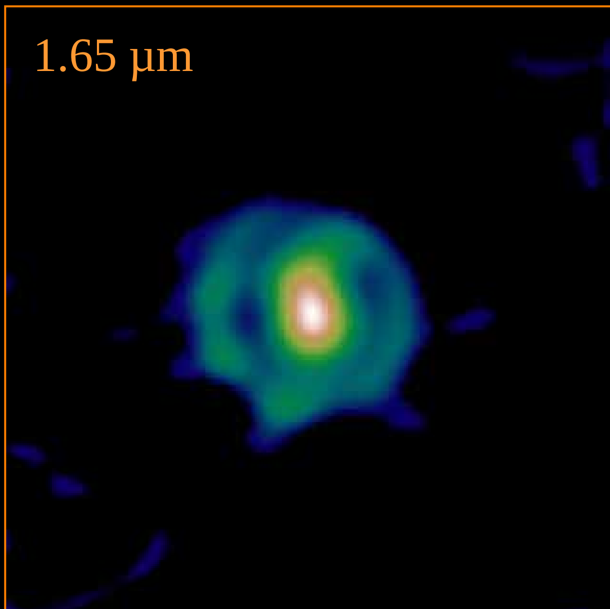

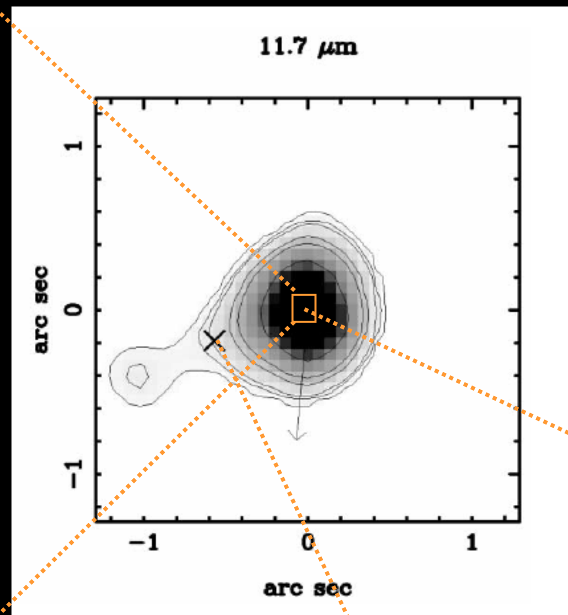

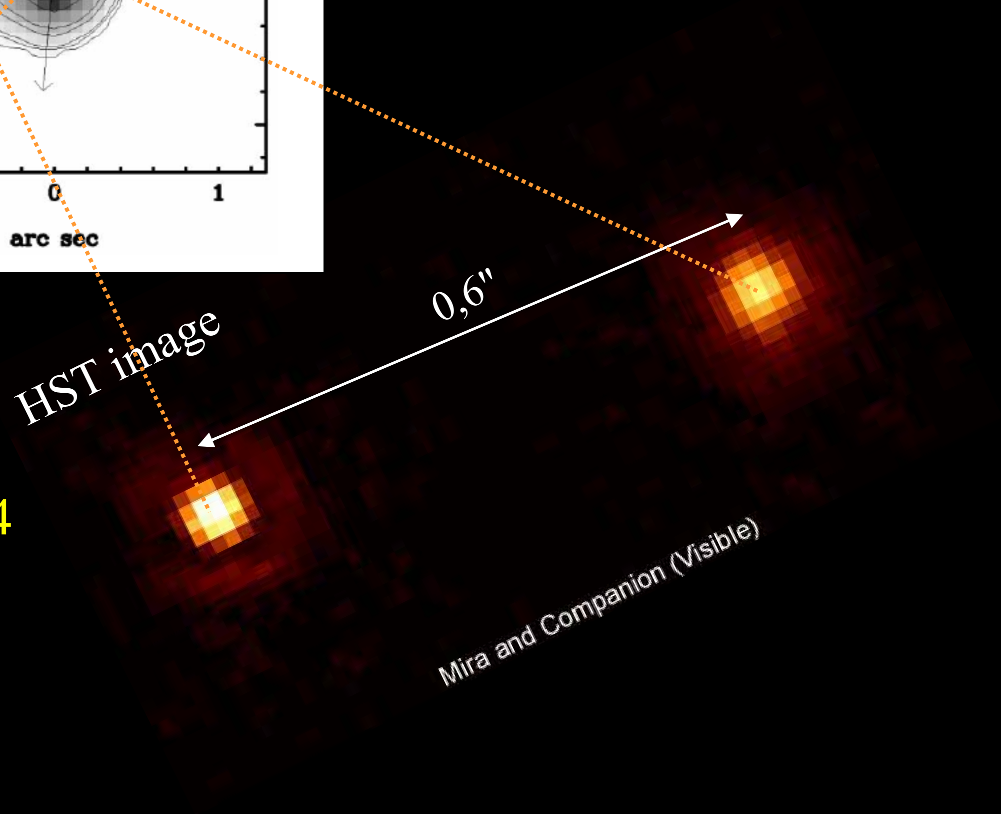

Gravitational darkening is excluded (by 4 orders of magnitude).